Repair of damaged parts by additive manufacturing

Hybrid (AM+SM) Manufacturing of metals

Bereket Angesom Abraha
Stian Bergan Høydal

Gradering: Åpen

Bachelor i ingeniørfag - Maskin
Innlevert: Mai 2023
Veileder: [Prof. Stergios Goutianos]

Norges teknisk-naturvitenskapelige universitet
Institutt for vareproduksjon og byggteknikk

NTNU
Institutt for vareproduksjon
og byggteknikk

Oppgavens tittel: Reparasjon av skadede deler ved additiv produksjon [Repair of damaged parts by additive manufacturing]	Dato: [22.05.2023] Antall sider: 69			
	Masteroppgave:		Bacheloroppgave X	
Navn: Bereket Angesom Abraha Stian Bergan Høydal				
Veileder: Prof. Stergios Goutianos				
Eventuelle eksterne faglige kontakter/ veiledere: Jostein Elnaes Thomas Bøe Jevnaker				

Sammendrag:
OnesubSea (OSS) Gjøvik har en interesse i å samarbeide med Nordic Additive Manufacturing (NAM) for å utvikle aditiv tilvirkning som en metode for reparasjon av deler. De vil se på eksempler fr to skader som har hendt på deler som er tilkoblet et kommisjonsprosjekt for testing av et desalineringsverk. Formålet er da å spare kostnadene på tilvirkning av nye deler, og i stedet reparere med 3D-printing.

Oppgaven består av analyse av to skader:

1. Sleeve Damage: en komponent har en toeransefeil på 1mm. OSS vil bruke additiv tilvirkning til å legge på 1mm materiale for å rett på toleransen.
2. Tool damage: en komponent har fått en skade fra uforsiktig bruk av verktøy, som har ført til en ripe i siden. OSS er interessert i å prøve ut additiv tilvirkning til å reparere skaden.

Stikkord:

Additiv tilvirkning
3D-printing
Hybrid tilvirkning
Reparasjon av defekte komponenter

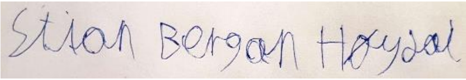

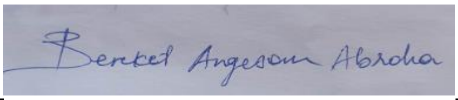

(sign.)

Preface

This bachelor thesis explores the utilization of additive manufacturing as a modern-day technique for repairing defects in super duplex stainless-steel parts. This research was carried out in collaboration with OneSubsea Gjøvik, a company that specializes in the advanced manufacturing of pipes and sleeves and involved the cooperation of the Nordic additive manufacturing (NAM) technicians responsible for maintaining and running the LMD machine. In addition, it was conducted under the supervision and guidance of Prof. Stergios Goutianos of NTNU Gjøvik.

The method used in additive repair is a subset of hybrid manufacturing, which works by combining additive manufacturing (printing) with subtractive manufacturing (machining, milling). While the primary focus of this thesis is utilizing the method to repair SDSS parts, a majority of the methods and numbers covered are relevant to hybrid manufacturing as a whole.

We would like to express our deepest gratitude to Professor Stergios for providing his expertise and guidance throughout the making of this paper. We are also immensely thankful to OSS, NAM & the material science lab at NTNU Gjøvik for their collaboration and provision of the necessary resources, as well as the expertise of their staff. Each and everyone have been very helpful in ensuring the success of this paper.

Lastly, it's our sincere hope that the findings of this study make a contribution to the understanding of using hybrid manufacturing for metal repair. The progress we have witnessed during the making of this paper has shown that this field of study has the potential to become very integral in the industry, and we believe that the topic itself is a goldmine for NTNU’s future bachelor students.

Gjøvik, May 2023.

Abstract

This bachelor's thesis inspects the use of additive manufacturing to repair two defects present in super duplex stainless-steel parts. The purpose of the study is to evaluate the effectiveness and reliability of hybrid manufacturing in the repair of these two defects and to evaluate whether it can be a possible alternative to traditional repair methods.

The thesis aims to carry out a thorough literature review of relevant research and technology within the additive production and repair of super duplex stainless-steel parts. Two potential methods for a repair procedure were found and documented: The first is a negative method involving 3D-scanning of a part to compare to a computerized 3D model, creating a negative model to use in the printing process. The second is a straight fill method involving pre-determined dimensions and filling an area up to a required volume.

A printing process and mechanical test were performed. The printing process was performed by a Laser Metal Deposition (LMD) printer on a block of UNS S32750 super duplex stainless steel to create a block of half-printed and half-parent material, which could then be machined into several specimens. A series of three tensile specimens were created and tested in a tensile machine to evaluate the performance of the repair method.

The results gathered indicate that LMD-printed material can have similar, or better mechanical qualities compared to hot-rolled UNS S32750 super duplex stainless steel, particularly in tensile and yield strength. Further tests would be required to determine the full range of mechanical properties inherent in LMD-printed super duplex, but the current results are fairly promising for a potential qualifying process of the LMD method as a hybrid manufacturing/additive repair technique, at least for super duplex parts. Further development of standards defining guidelines for repair procedures could enable the implementation of the LMD printing for additive repair in the near future, which will likely help reduce the costs of repairing defects in manufacturing and failures during installation.

Table of content

Picture list

Table list

Figure list

List of abbreviations

Abbreviation	Definition
OSS	OneSubsea
NAM	Nordic Additive Manufacturing
SDSS	Super Duplex, Stainless Steel
CAD	Computer-aided Design
CNC	Computerized Numerical Control
SLM	Selective Laser Melting
EBM	Electron Beam Melting
LMD	Laser Metal Deposition
DLD	Direct Laser Deposition
AM	Additive Manufacturing
SM	Subtractive Manufacturing
HM	Hybrid Manufacturing
HR	Hot Rolled
PLA	polylactic acid
PETG	Polyethylene terephthalate glycol
ABS	Acrylonitrile butadiene styrene

List of symbols & units of measurement

Symbol	Unit	Definition
σ	MPa	Stress
F	N/kN	Force
A	mm^2	Area
ε	(Ratio)	Strain
m_E	GPa	Young's modulus
$R_{p0.2}$	MPa	Offset yield strength
R_m	MPa	Ultimate tensile strength
F_m	kN	Maximum force applied
A_g	%	Elongation
a_0	mm	Thickness
b_0	mm	Width
S_0	mm^2	Cross-sectional area

Glossary

Glossary	Definition
Parent material	The original, unprinted material used in tests, i.e UNS S32750 SDSS. round bar steel. Term used specifically for this paper.
Printed material	Refers to the material deposited by the LMD-printer. It is material created with AM methods.
Weld point/ binding	Refers to the area where parent material and printed material meet.
Inter-layer time	Time between deposited layers in 3D-printing.
Bridging	A process filament printers use to cross an air gap in a model by laying the material across like a bridge.

1 Introduction

Super duplex stainless steel (SDSS) is a type of steel with a microstructure that consists of 50% austenite and 50% ferrite. SDSS offers outstanding corrosion resistance and high mechanical strength, typically up to ≥550MPa offset yield strength, and ≥750MPa ultimate tensile strength. This makes SDSS ideal for use in harsh environments, such as those found in the oil and gas industry, as well as marine and chemical processing applications, (Smithmetal.com, 2020). However, SDSS materials are still subject to defects that can compromise their integrity and reduce their lifespan, despite their outstanding properties. For example, the two defects that occurred in SDSS components are length measures under the minimum tolerance (lack of material) and surface scratches resulting from tool damage.

To ensure their performance and safety, repairing these defects in SDSS components is essential. When it comes to SDSS materials, traditional repair techniques, such as welding and brazing, have limitations. for example, welding can result in microstructural changes and corrosion issues in the welded zone and heat-affected zone, while brazing can result in cracking and reduced mechanical properties. As a result, there is a need for other repair techniques that can maintain the mechanical properties and corrosion resistance of SDSS components. And in this case, it’s chosen to use 3D printing.

Additive manufacturing (3D printing) is a promising technology that offers a wide variety of new opportunities and benefits by enabling the production of complex product designs, rapid innovation and improved economics for lower-volume production and customization. This technology involves creating an object by building it one layer at a time. Additive manufacturing has several advantages over traditional repair techniques, including the ability to repair complex geometries and reduce material waste, (NIST, 2022).

In this study, we investigate the use of one additive manufacturing technique, laser metal deposition (LMD) for repairing two different defects; an object that is lacking material and is therefore too short to satisfy the minimum tolerance requirement, and an object damaged by a tool, resulting in scratch damage on the surface. The repairs are intended to be done on SDSS components, so material composition is also important. To evaluate the effectiveness of this technique we compared the mechanical properties of the repaired samples to the material qualities of standard UNS S32750.

1.1 The problem

The task given by OneSubsea was to investigate the possibility of repairing two different defects in a mechanical part utilizing additive manufacturing, define potential methods to be used as repair procedures, and determine the possibility of qualifying LMD-printing for standard use in repair operations. Each problem poses a different challenge to repair

1.1.1 Problem #1: Surface scratch caused by tool damage

The first problem, a machined part experienced damage to the surface as the result of the accidental tool, resulting in a deep cut in the surface of the material. This defect presents the challenge of requiring some means of filling in a small gap that binds with the surrounding material, dealing with the uneven dimensions of a damaged area, as well as taking into account deformations in the metal; a topic we will discuss later.

Picture 1: Surface scratch on a part (J. Elnaes 2023, personal communication, 15 May).

1.1.2 Problem #2: Tolerance error/Lack of material

The second problem presented would be a small lip on the inner circle of a tube that had been machined down 1mm lower than the required tolerance. This defect poses the challenge of filling in a surface up to a required dimension. For the purposes of being thorough, we also considered that the surface in question could have been uneven, and not a simple flat plane.

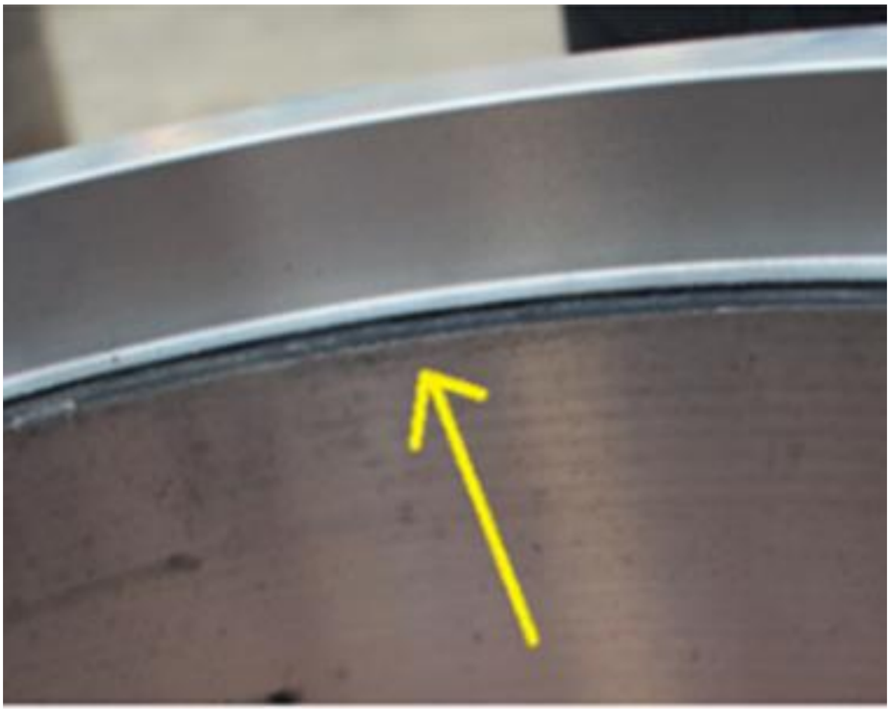

Picture 2: Lack of material in part (J. Elnaes 2023, personal communication, 15 May).

1.2 Differences between AM and SM

1.2.1 Subtractive Manufacturing

Subtractive Manufacturing (SM) refers to methods that utilize techniques to remove/subtract material from a larger mass of material until you are left with a part possessing the desired dimensions and specifications required. Methods include milling, cutting, grinding, stamping, machining, injection molding, and more. (Dassault Systèmes, 2022)

1.2.2 Additive Manufacturing

Additive Manufacturing (AM) refers to methods that utilize techniques to deposit/add material together to build an object up to the dimensions and specifications required. In this paper, we will be discussing methods relevant to the subject matter, though many may already be familiar with methods from commercial printers such as filament-based printing using polymers such as PLA, PETG, and ABS, or resin-based printers.

1.2.3 Hybrid Manufacturing

Hybrid Manufacturing (HM), as the name suggests, is a combination of Additive and Subtractive Manufacturing to achieve a final product. The types of manufacturing used can be in any order, even multiple times over. As a running example, one could start with a block of steel, milling the initial outline for an engine block, 3D-print the advanced geometry required for the part, then come back and machine the surface to the required tolerance.

In the context of this paper, we will primarily discuss the usage of HM as a repair method, meaning it will be utilized to repair objects typically created by subtractive methods. However, keep in mind that most methods mentioned in this paper also apply outside of repair as well, and can be used in planning a HM process.

2 Theory

2.1 How metal-based AM works

Metal-based printing is a technology that creates 3D metal objects by adding layer by layer of metal powder using an electron beam or laser beam. The process starts by creating a digital model (3D) of the main object. To do that, man can use CAD (computer-aided design) software or a 3D scanner (for scanning an existing object). Then, the created model is imported into the metal-based printers' software, which slices the model into thin horizontal layers. Then these layers are printed layer by layer until the final object is complete.

The printing process starts by filling the build chamber with inert gas (for example argon) to minimize the oxidation of the metal powder and then it is heated to the optimal build temperature. A thin layer of metal powder is spread over the build platform and a high-power laser scans the cross-section of the component, melting (or fusing) the metal particles together and creating the next layer. The entire area of the model is scanned, so the part is built fully solid. When the scanning process is complete, the build platform moves downwards by one layer thickness and the re-coater spreads another thin layer of metal powder. The process is repeated until the whole part is complete. When the build process is finished, it is supported by a series of support structures that help keep it stable and prevent it from distortion that may occur due to the high processing temperatures. After it cools down, it is cleaned and polished to remove any excess metal powder (Hubs, 2023).

2.2 Classification of different AM methods for metals

There are several classifications of metal-based additive manufacturing. Each method has a different approach to creating and binding the material into a solid object, with different strengths, weaknesses, and applications.

The one that will be discussed in this particular thesis is the LMD method, as it has several benefits that will be discussed later.

2.2.1 Selective Laser Melting (SLM)

Selective laser melting is one of the laser powder bed fusion technologies. It is a laser-based 3D printing technology in which metallic powder materials are selectively melted layer by layer to produce 3D objects in nearly any shape (Voxeljet, 2022). SLM can be used to produce objects using various metals with a high density.

The process of printing begins by uploading a file of the desired model to the project portal and choosing the quality material and finishing. Then, the software divides the file into layers and sends them to the printer in the form of instructions. This method uses a laser to melt the metal powder which then cools and solidifies. Each laser cycle produces a new slice of the object, then the work platform is lowered by exactly the thickness of one slice and a scraper redistributes the powder. the melted metal solidifies, and the process is repeated. The old and new layers are fused together by the laser until the object is completed. Each component is welded to the work platform with a support, which is detached after the component is removed. The finished object is removed from the unused recyclable powder and freed of excess powder. The process results in very rugged precision of manufactured objects.

Selective laser melting really helps when complex components need to be produced in a short time. It also implements the production of complex products with integrated functional elements such as conformal cooling.

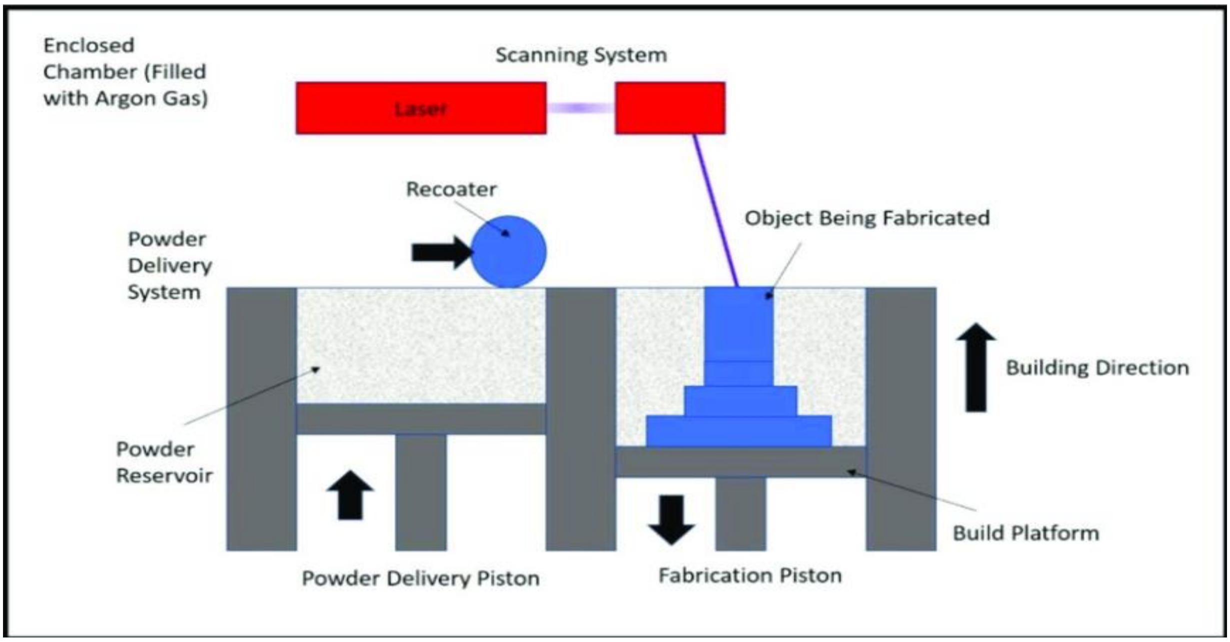

Picture 3: Diagram of SLM process (ResearchGate, 2018)

2.2.2 Electron Beam Melting (EBM)

EBM is a powder bed fusion process in which each thin layer of metal powder is deposited onto a heated bed and then melted or sintered into place. However, EBM differs from other processes in that the energy source that fuses the powder is an electron beam instead of a laser beam, and the process takes place under a vacuum instead of atmospheric pressure (Team Xometry, 2022).

EBM typically takes place inside a machine under a vacuum at very high temperatures. The process of printing starts by spreading a layer of metal powder across the build area, then pre-heat all that powder and using the electron beam to fuse it together and melt it together just in the places where you need to build up your part. This process repeats over and over until it eventually ends up with something like a semi-solid block or cake of powder that contains all the preheated powder, regardless of whether or not it was melted with the solid parts inside. These parts need to be broken out and de-powdered before continuing with the rest of the workflow.

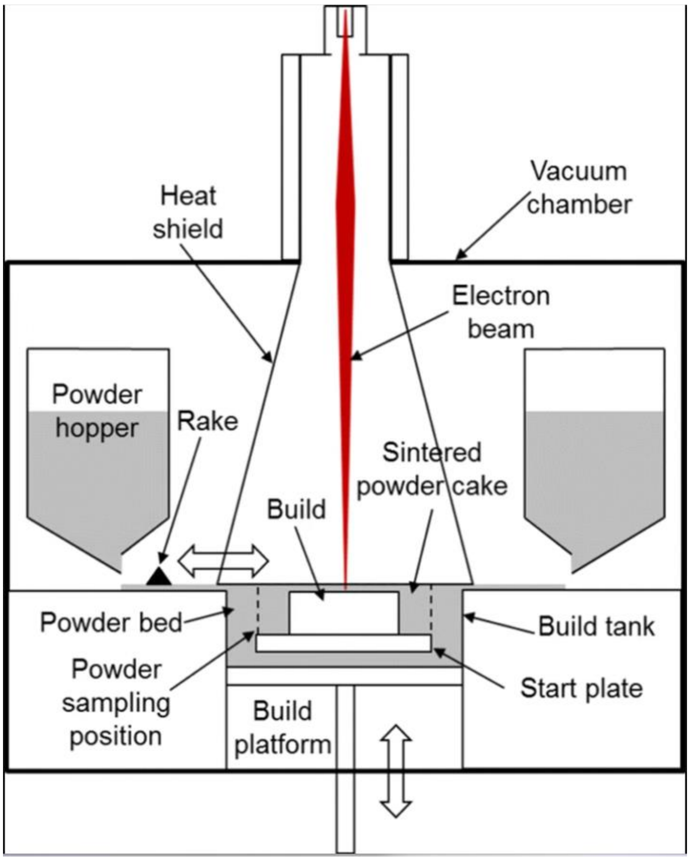

Picture 4: Diagram of EBM process (Gruber et al., 2019)

2.2.3 Laser Metal Deposition (LMD)

LMD is an additive manufacturing process in which metal is heated by the laser and deposited onto a metallic substrate, layer by layer, and it is used to manufacture, strengthen, and restore parts (American Cladding, 2022). LMD printers use a laser to melt the metal powder and create the desired object layer by layer. The process starts with powdered metal, which is fed into the nozzle and safety gas (typically argon) is connected. This safety gas prevents metal oxidation during the printing process. After the metal powder is fed to the nozzle, the powdered metal is deposited into the melt pool under the laser, where it combines with the base material into a metallurgical bond. The process is repeated layer by layer until the final design/repair is complete. To control the movement and intensity of the laser, a computer program is used.

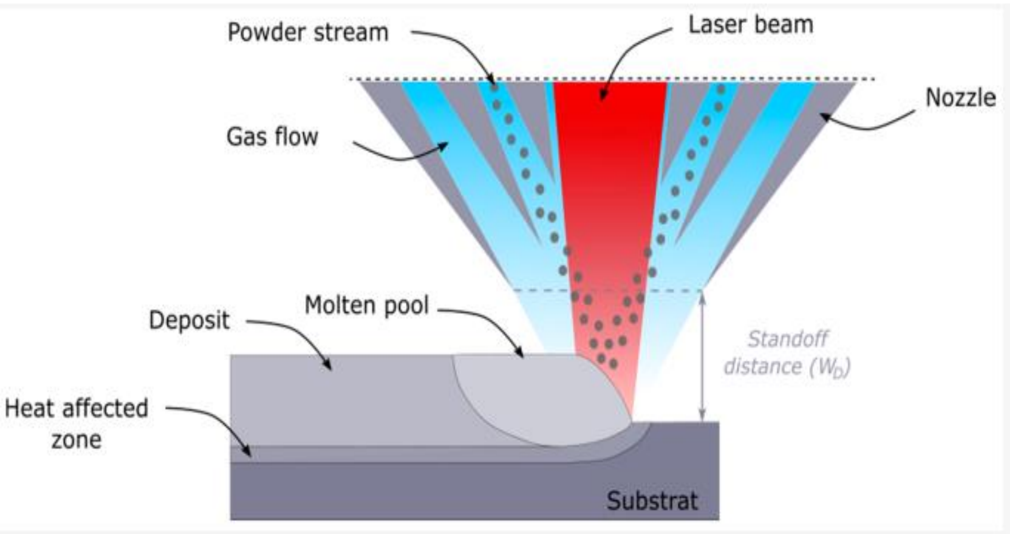

Picture 5: Diagram of LMD process. (Ferreira et al., 2020)

2.3 Benefits of LMD-printers in hybrid manufacturing

There are several benefits to utilizing LMD in combination with subtractive manufacturing methods such as machining, especially in the repair of damaged parts. This section will also discuss some dissimilarities between LMD and filament-based polymer printing, to hopefully dissuade perceived misconceptions from previous experience with AM methods. Do note that some specifics of these features are dependent on the model and type used. Much of the knowledge written here is based on the TrueLaser 3000 LMD printer. There may be key differences, depending on the specifications of the model you use.

2.3.1 Relative cost

Make no mistake, while the costs of AM are becoming cheaper as the technology is further developed and better understood, it is not an entirely inexpensive solution. However, the relative costs of repair with AM, compared to the potential costs of replacing a damaged part with a brand new one, is enough to make the method a worthwhile consideration.

To draw an example from the ongoing collaborative project, the costs to replace a particularly large and complex part machined out of Super Duplex can be between six to seven figures, whereas repairing the damage with AM could cost as low as four to five figures, depending on the size of the damage (values mentioned are estimated in Norwegian Kroner).

There is also the consideration of saving time. There is no quantifiable way to consider the potential costs incurred by project delays caused by damaged parts. However, depending on the importance of the part in question, spending several months acquiring a completely new piece could incur further project costs that are immeasurably expensive, when the alternative could be utilizing AM methods to perform a repair in the measure of weeks, or days, depending on the complexity.

2.3.2 Material composition

When it comes to additive manufacturing, it is important to talk about material composition, as there is a huge difference in the material structure present in conventional consumer printers, compared to LMD-printers. The composition of a 3D-printed structure utilizing polymers such as PLA and PETG will usually result in a layered composition, with layers deposited parallel to the print bed (typically horizontally). This will result in a construction that is typically only strong in one direction, and fragile or significantly weakened in the other.

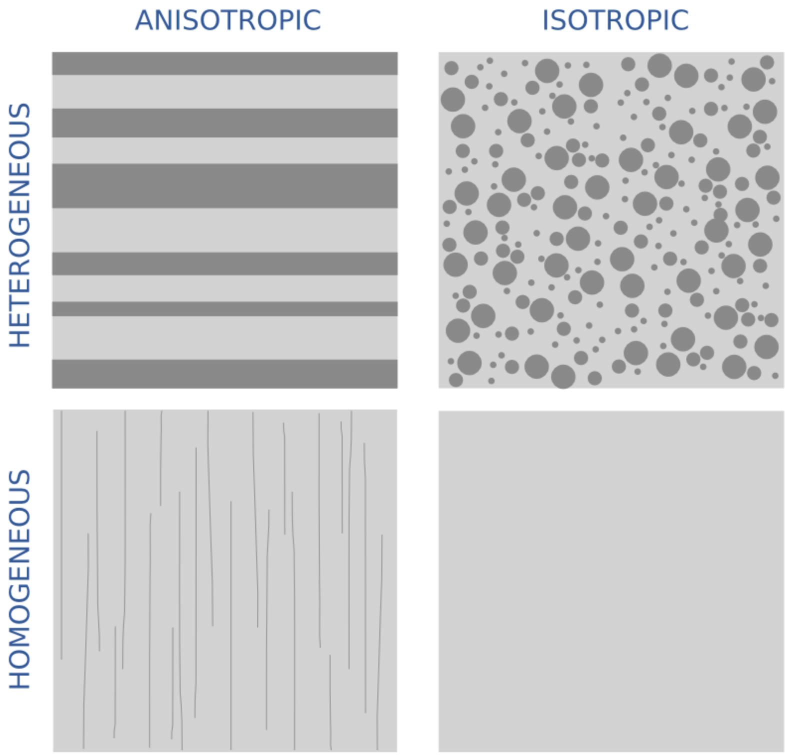

Picture 6: Different states of material composition. (Hall, 2015)

Such is not the case with LMD printing. Due to the method being more similar to welding, the composition of an LMD printed part is typically more homogenous, rather than layered. Studies on different metal types such as 316L stainless steel show that DLD (a different name for LMD) printing methods tend to result in improved mechanical properties, such as higher ultimate tensile strength and yield strength, compared to their cast and wrought counterparts (Aref Yadollahi et al., 2015). This is, however, very dependent on the selection of methods used during the process. Poor methods can result in Anisotropy in the printed material, which will reduce certain mechanical qualities.

2.3.3 Construction complexity

AM is capable of creating shapes that are typically far more complex than what can be replicated with most subtractive methods. However, someone with experience using resin or plastic-based consumer printers may have the predisposition to think a certain way about printing complex geometry. Because consumer printers typically tend to build their shapes from the ground up, features such as overhangs and gaps can be very challenging for 3D printers, and typically require using methods such as bridging and/or using support materials to increase the complexity and cost of repair.

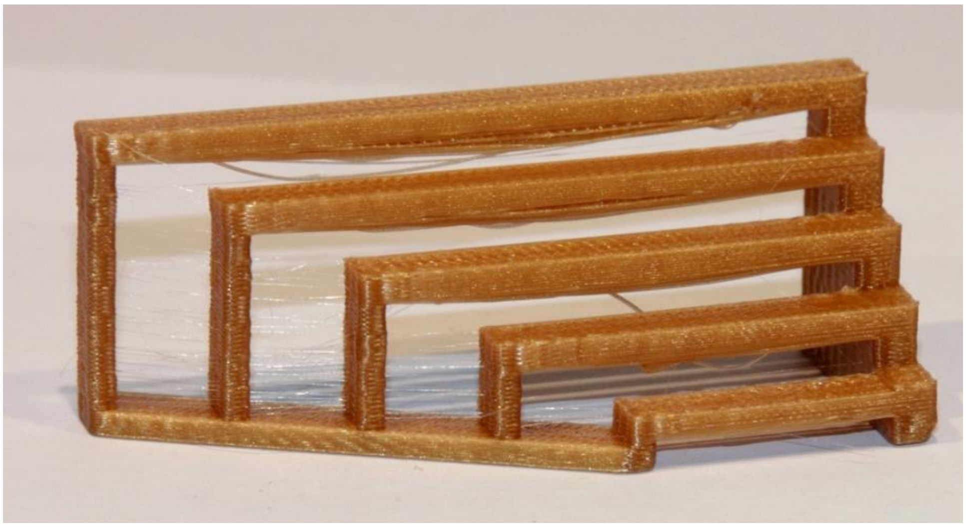

Picture 7: Bridging in filament-based printers. (Washington.edu, 2017)

This is a non-issue when dealing with industrial LMD-printers, which tend to have multiple axes of movement. In an interview with a NAM technician, they stated their LMD machine uses 5 axes of movement, allowing the machine to orient the substrate (work area) horizontally (M. M. Vik 2023, personal communication, 3 May). Using this feature, the machine can continue to print vertically throughout the entire build process. This eliminates the need for any additional support structures, as it can utilize the area it is working on to support the build until the melt pool solidifies.

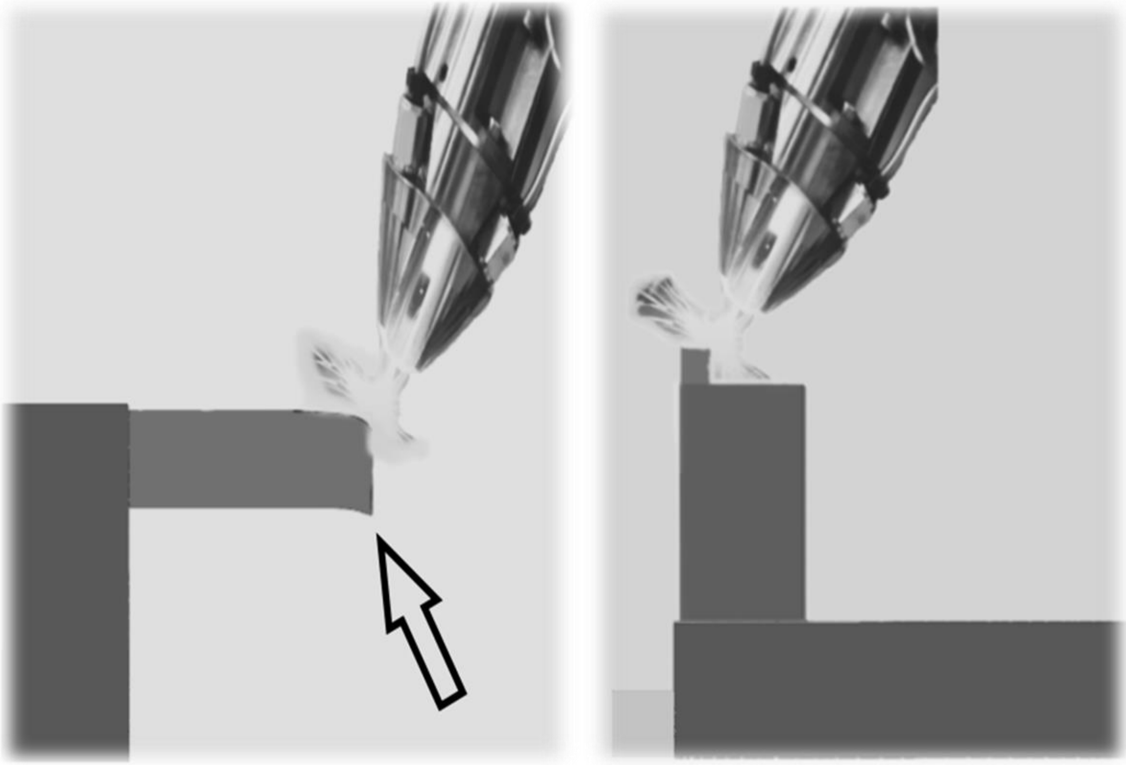

(a) *(b)*

Figure 1 (a&b): Orienting the build surface to be horizontal to gravity. illustrative purposes only

2.4 Considerations for an AM repair procedure

This section discusses potential challenges to consider when planning to perform an additive repair. It is worth adding as a disclaimer that many of the limitations talked about below, exist at the current time of writing. Additive manufacturing, and especially hybrid manufacturing, is a relatively new technology and rapidly developing. It is quite likely that many of these issues will be mitigated or even become irrelevant in the future. Some issues are also model-dependent and must be considered in light of the tools utilized for the planned task.

With all that in mind, let us talk about what should be considered when planning out the repair of a damaged object, and in which situations it may be unideal to utilize additive methods to conduct a repair.

2.4.1 Precision & tolerances

AM methods are capable of complex shapes with fairly high precision. For the machine that was used during testing, technical documents state an accuracy of 0.015mm in the linear axes XYZ, and a 0.02-degree accuracy in rotary axis B (Trumpf.com, 2020). It is possible to have fairly small layer heights, however, high-precision prints require particularly small layer heights, with incredibly precise spot sizes. Smaller spot sizes mean smaller layer heights, and smaller layer height means slower progress per layer. This means that extremely precise printing will take more time to complete, increasing costs.

From the interview, and confirmed in email correspondence with both NAM technicians, it was stated that while the machine can print with very high precision where required (M. M. Vik, T.B. Jevnaker 2023, personal communication, 12 May). However, for very fine tolerance requirements, it is easier to use less precise tolerances in the AM process, and later use subtractive methods to reach the required tolerances where applicable. The specific number is usually determined on a case-by-case basis, but a typical tolerance lies usually at around 0.2mm.

2.4.2 Deformations prior to repair

When planning out a repair procedure on a damaged metal part, it is important to consider the potential deformation in the material caused by the damage inflicted on the part in question. Such damage may have altered the mechanical properties in the local area, particularly in the form of residual stress, changes in the crystal structure, or microcracks (Noyan and Cohen, 1987, p.152; Industrial Metallurgists, 2016).

Defects such as these can potentially be harmful to the part in the long term if it is not handled prior to starting the repair process. Consider removing excess material around the damaged area prior to commencing repair by way of milling/machining. This will also aid in simplifying the surface geometry on the substrate, making the repair process easier.

2.4.3 Contaminants

While surface adhesion on the surface boundary is not much of a concern in LMD-type printing, one thing that is extremely important to consider before beginning repair on a surface is the cleanliness of the surface in question. According to an interview with one of NAM's technicians, contaminants present on the substrate can result in poor binding between the printed material and the parent material (M. M. Vik 2023, personal communication, 3 May). This could cause structural weaknesses at the weld point between the two, which could eventually lead to failure below the expected load of the material.

It is therefore important to consider proper decontamination of the area before beginning the AM process. According to the NAM technician, it is considered good practice to mill out smaller cracks and nooks before cleaning, to ensure they are properly decontaminated before commencing the AM process on a workpiece.

2.4.4 Clearance

When planning the repair of a damaged area within an enclosed space, it is important to consider the clearance of the machine, to make sure it is able to reach the area intended for repair. Per correspondence over email, the NAM technician recommends maintaining a space of roughly 2-3mm clear around the nozzle, ensuring some margin of safety (M. M. Vik 2023, personal communication, 8 May). This number will vary depending on the model used, and the depth that the nozzle is required to enter to perform repairs. LMD printers such as the one used for this test have a high degree of freedom to navigate objects, so long as it has the necessary space and angle to do so. For spaces smaller than the machine can access, solutions will need to be discussed on a case-by-case basis.

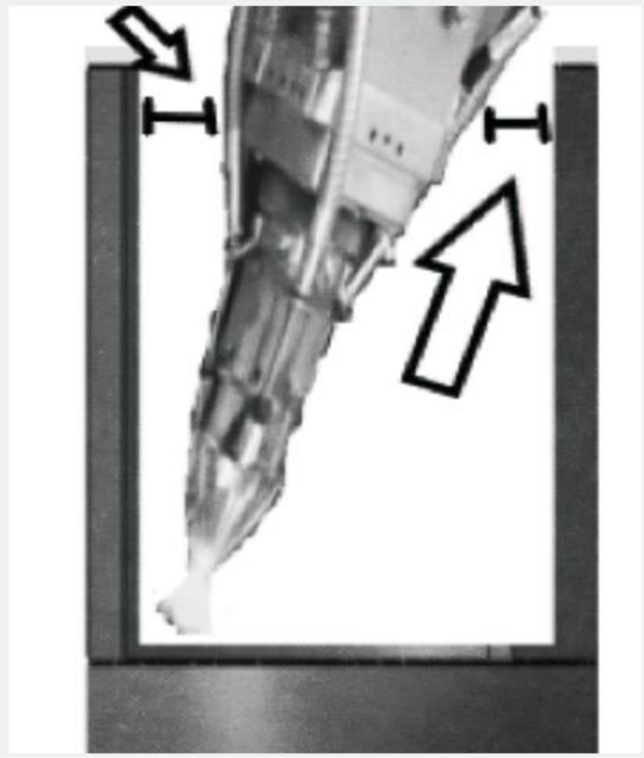

Figure 2: Nozzle clearance in an enclosed space. the figure is for illustrative purposes only.

2.5 Discussing potential repair procedures

In order to repair a part, two primary methods were suggested and discussed with the technicians at NAM. Both were deemed viable, each providing different benefits and drawbacks to their use.

Regardless of the method used, it is still recommended to prepare the surface with methods such as machining, flattening the area, and reducing the risk of contaminants in or on the substrate. This should always be the proceeding steps of any repair procedure.

2.5.1 Fill method

This is the most straightforward method, the fill method involves simply filling in the missing material atop the part, building up the surface to a required amount. The piece would then be machined to the required tolerance afterward.

The fill method should incorporate preparation of the surface to accommodate for an even fill. The intended repair area should be milled or machined to a certain set dimension, simplifying the process of matching the repair to the intended surface. Preparing the surface will also help in removing contaminants from the area, which is critical to ensure proper binding between the parent material and printed material.

This repair procedure is rather simple to implement, with few required steps. It is a very cost-effective method, trading accuracy for efficiency. This is the primary method that will be used during the creation of test specimens, as it is cheap and easy to perform.

2.5.2 Negative method

This would be a more advanced method. If the part in question has a corresponding CAD model that can be used, this method can be used to rebuild the part according to the CAD model. Utilizing a 3D-scan of the model by way of a CT-machine or other measuring tools, one could utilize CAD software to compare the part as-is, to the intended dimensions of the model, and create a negative of the model. This negative can then be utilized to create a build solution that can accurately rebuild the full model. Software capable of comparing 3D models to 3D-scans already exists, making it a viable option for making negatives to be used in 3D-printing.

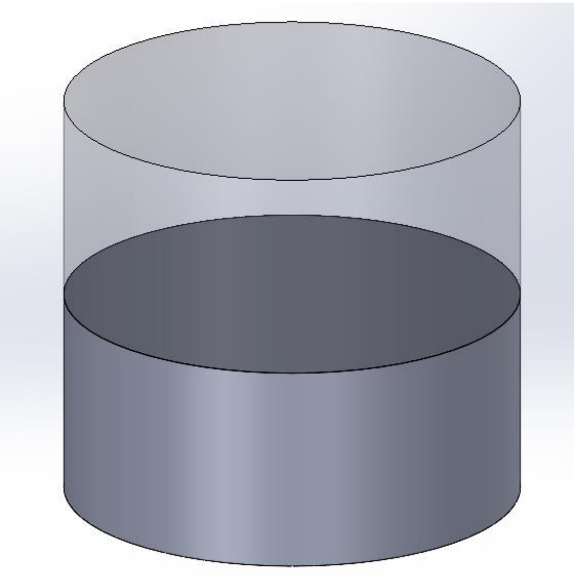

Figure 3: A cylindrical CAD model split in half to illustrate how one can create a negative from a scan.

Despite allowing for the creation of a build solution that incorporates more uneven/complex build surfaces, the area of intended repair should still be prepared in order to remove the possibility of contaminants on the substrate getting into the melt pool and endangering the structural integrity of the weld point.

This method is more costly but could be useful for building up areas that have uneven surfaces, features that have complex geometry, or that presents any other challenges that might make a simple fill deposition ineffective for repairing the part.

2.6 Proposed experiments to test material quality

In order to test the viability of both AM as a method, and the repair procedures considered, several different experiments were proposed. Ultimately, most were dismissed in favor of a single solution. There were several mechanical tests that could be used to test the qualities of the repaired material. However, it was ultimately settled on by all parties that the mechanical tests which would yield the most useful data for qualifying a potential repair method, were tensile testing and impact testing. These experiment suggestions would be built around the plan of creating Specimens for these two tests.

All of the proposed solutions below would utilize the fill method, as this would be the cheapest method to test, and the complexity of a negative method would not be useful in a lab setting for now.

2.6.1 Lack of Material: Building up material

This hypothetical test was suggested in order to test either of the two methods. The experiment would be done by machining a coin-sized test piece using UNS S32750 SDSS, and ignore all tolerances to create an uneven surface, and applying either of the two suggested repair procedures to repair the test piece up to 1-2mm.

This test was deemed unnecessary, due to the similarity in the repair method used for the practical experiment that was ultimately chosen, meaning the experiment would not yield any useful information not already covered.

2.6.2 Tool Scratch: Induced damage

A suggested method of testing repair methods was to artificially induce a tool scratch onto a plate of material, either by manual use of a tool, or careful use of a Charpy machine at a set force, to induce a realistically damaged test sample of which to use to create specimens.

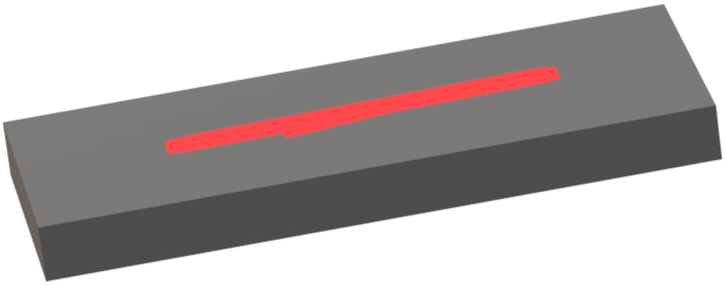

Picture 8: The specimen is inflicted with an unevenly dimensioned scratch.

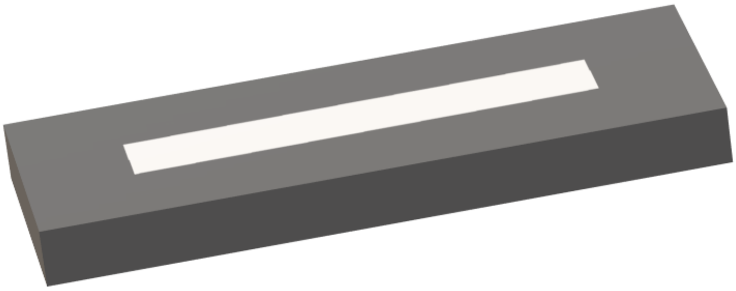

Picture 9: The specimen is then milled and repaired in a set dimension.

After the damage was induced, there would be two options:

- Fill in the area as is and test the damage with the deformations included to see the results of improper repair procedures.
- Mill out the area surrounding the scratch and perform a proper repair procedure, testing the material quality.

Regardless of the method used, the idea of this test was to realistically simulate creating a tool scratch in a lab setting, to see what the different parameters could tell us. This test was scrapped because it would require too many test specimens to be properly tested, something that would be very expensive and not present much end-value for OSS.

2.6.3 Tool scratch: Milled damage

This test is similar to the induced damage test, except that it skips past the induced damage, going right to milling a hole in the plate Specimen and filling in the hole with the material. The Specimen would then be tested.

This method was primarily intended for tensile tests, though a similar Charpy test would have also been used.

2.7 Practical experiment: Half-fill material

This is the experiment that was ultimately settled on.

The premise for this test is simple: Half the specimen would consist of a block of steel bar, while the other half would consist of deposited material from the LMD printer. The material would be printed onto the block directly, after which a sample would be cut out from the half-block, half-print, and turned into test specimens.

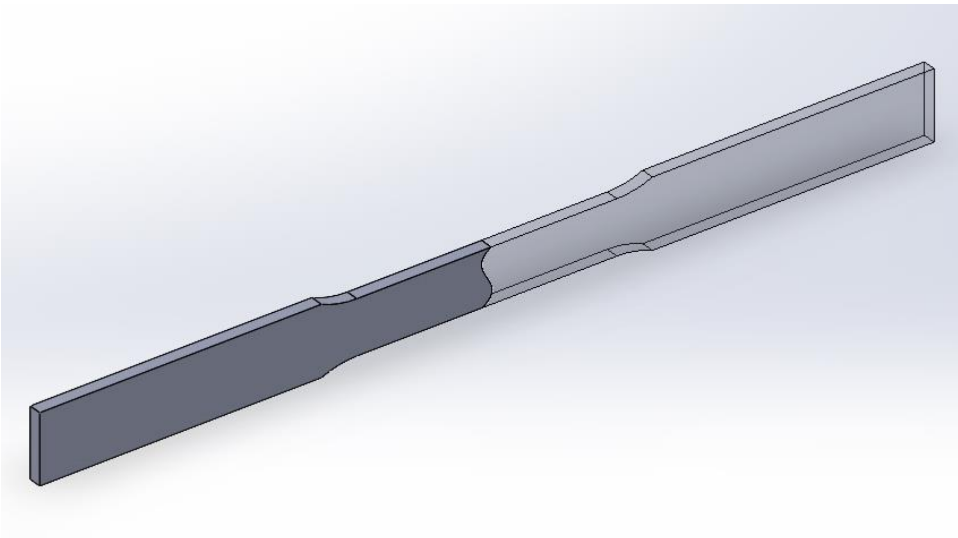

Figure 4: The specimen is divided into two halves (half original block and half printed).

2.7.1 Benefits & considerations

This method simplified the creation process of specimens, as the acquired test material could be much shorter than the required dimensions for the planned tensile test, which had a requirement that the grips be at least 65mm minimum, so as to not damage the tensile machine. With this method, the acquisition of the test material would be much easier, as it could use a smaller block of SDSS, saving time and resources.

The other benefit of using this method is that the balance between materials leans more evenly between the parent material and the printed material, putting a heavier burden on the printed material half, which would provide a better understanding of its material qualities.

For the tensile test, the point of failure will now provide more information on the difference in material quality between printed and non-printed material, depending on which side of the specimen breaks first, and if the breakage is brittle or ductile. This may not be a strong indicator of all qualities of the material, but it can provide insight into some key differences between the materials.

Finally, this arrangement will also help test the boundary between printed and non-printed material, which is now situated in the middle of the specimen, thus ensuring that the binding between the two is sufficiently strong. Should the breakage happen in the middle, it could suggest poor binding between the two materials.

2.7.2 Specimen size and standard

After further discussion on the viability of the test and the material available to do the job, it was ultimately agreed to settle for a tensile test with 3 specimens, where half the piece would be cast metal and half 3D-printed material. The test would be done using the DNV-ST-B203 standard (DNV, 2023), which refers to ISO 6892 (Standard.no, 2019) as its reference standard for tensile tests.

A Charpy impact test utilizing the ISO-148-1 standard (Standard.no, 2016) was also planned, but due to several setbacks, such as time and lack of test equipment during the planned test period, this test was scrapped. The intended method will still remain.

2.7.3 Dimensions

For this test, a flat dog bone test piece was selected, as per ISO 6892, Annex B. It would have a thickness of 3mm, and a width of 12.5±1mm at the test area, as pictured below. Machining tolerances would be according to Annex B, which is about ±0.05mm. The final dimensions are as shown below.

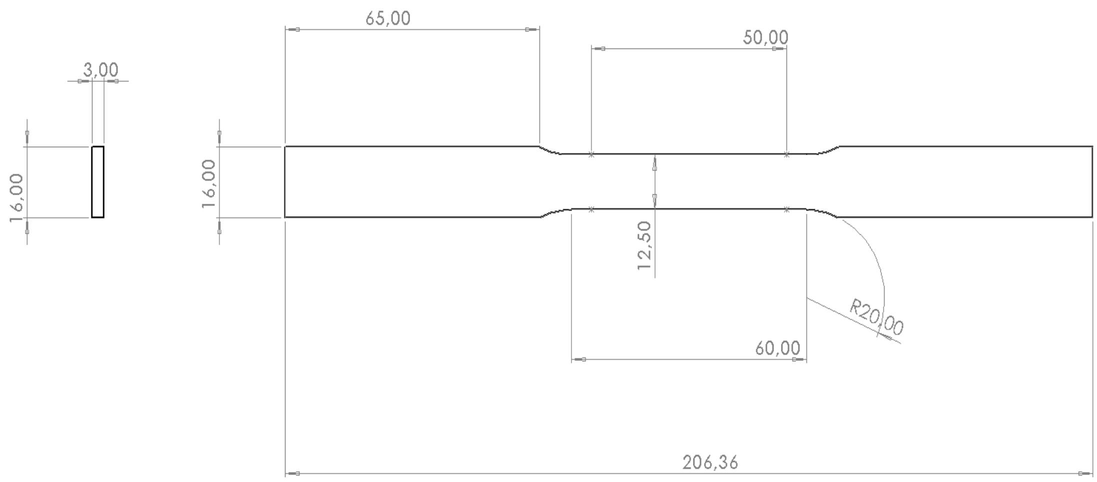

Figure 5: Specification of tensile specimen

2.7.4 Calculations

The machine that would be doing the test has a maximum load of 100kN, with an ideal load of about 40-50% of the maximum. The material we plan to use, UNS S32750 SDSS, is known to have a minimum ultimate tensile strength of 750 MPa. To ensure that the planned test was within these parameters, the following calculations were made:

Cross section of the test-piece at maximum tolerance

$$A_{max} = 13.5mm \times 3mm = 40.5mm^2$$

Expected tensile strength

$$\sigma \geq 750MPa$$

Maximum required force

$$F = \sigma \times A$$

$$F(N) = 40.5mm^2 \ \cdot 750MPa$$

Simplified

$$F(N) = 30375N \Rightarrow 30.375kN$$

Given these calculations, the test will only incur a maximum of 30.4% load on the tensile machine and is therefore within acceptable limits. The test plan was submitted to the lab and approved.

3 Case/Materials

3.1 Material

For the project, the material provided for testing was two blocks of HR round bar of UNS S32750 Super Duplex steel. The first was a small cylindrical block with dimensions 100mm diameter, and 29mm height. The second was another cylindrical block of 110mm diameter, and 72mm height. The blocks that were provided have previously been certified up to the 750MPa minimum requirement, and as such, this would be the expected tensile strength to meet for the repair attempt to be considered a success.

Wärmebehandlungszustand / Condition of heat treat: lösungsgeglüht / solution annealed
gem./acc. to ASTM A182: 1100°C 2,5h Wasser/water - Abkühlung/cooling < 260°C

Probe-Nr. Test-No.	Lage loc.	Temp. °C	Rp0,2 N/mm²		Rm N/mm²	A4 %	Z %	Kerbschlagarbeit Impact value J	Probenform Shape of test piece Charpy-V °C	Härte Hardness HRC
Soll/Req.	L	RT	>=550		>=760	>=25		>=45	-46	<=32
	T	RT	>=550		>=750	>=25		>=45	-46	
007MM1	L	RT	577		790	44	77	283 292 289	-46	23

Anlagen Encl. US-Protokoll/UT report	Freital,den Place and date	Abnahmebeauftragter Inspector representative

Picture 10: Certificate of the provided material. (J. Elnaes 2023, personal communication, 15 May)

Both materials were provided for free, as part of the testing. There is some ambiguity on whether or not the round bar is actually HR or not, however, all the information available on the block suggests that it is. As such, it will be considered one for comparisons between the parent material and printed material.

3.2 Equipment

3.2.1 Printing

For producing the samples, a Trumpf Truelaser 3000 would be available to take care of the actual printing process. This is a machine capable of attaching three separate modules: A laser cutter, a laser welder, and an LMD laser (Trumpf.com, 2020). For the purposes of this test, only the LMD-printer module will be relevant.

The machine is an enclosed (not airtight) chamber, which utilizes inert gases such as Argon to create an inert atmosphere within the build-chamber, preventing oxidization during the printing process. Depending on the requirements of the metal, Nitrogen can also be used instead of Argon. Additionally, according to an interview with the NAM technician, the manufacturer of TrueLaser 3000 recommends helium as the driving gas for the metal powder itself (M. M. Vik 2023, personal communication, 3 May).

The machine uses two or more hoppers, which feed the machine with metallic dust specifically made for printing, the dust then travels through hoses to the nozzle, which deposits the material on a surface while the laser creates a melt pool localized on a fine point called a spot. This spot size is determined by the laser focus, which can vary depending on the model and which nozzle is utilized.

The Truelaser 3000 has 5 axes of movement. As mentioned previously, the positional accuracy of this model printer is 0.015mm in the linear axes XYZ, and a 0.02-degree accuracy in the rotary axis B (Trumpf.com, 2020). From an interview with one of the NAM technicians, the Truelaser 3000 has a freedom of 360 degrees to move, with the in-built software limiting the range to 120 degrees while the LMD module is installed (T.B. Jevnaker 2023, May 19).

Picture 11: TruLaser Cell 3000 (3D printer)

This particular machine also features redundancies and safety features such as safety glass to keep fumes and particulate matter from entering the laser optics, shielding the optics from splatter and debris.

3.2.2 Testing

For testing tensile specimens created from the material sample, a tensile machine would be needed. The currently available tensile machine available at NTNU's B-lab is a 100kN, Zwick Roell machine, which according to an interview with the laboratory manager, is refurbished from an older Karl-Frank tensile machine (K. Kalvåg 2023, personal communication, 15 May). Because the machine is not an existing model, but a refurbished variant of an older machine, no accurate technical documentation exists, though it features most of the common fittings of a Zwick Roell machine. It comes with an extensometer, load cells, control panel, safety glass door, and its own digital software, testXpert.

Picture 12: Tensile machine in NTNU

This machine is used to test a variety of material qualities within a tensile specimen, such as yield strength, ultimate tensile strength, and elongation of the specimen. This data will be useful for determining the quality of the printed material in the planned test. The extensometers have the ability to test the elongation within the gauge length of the specimen, giving a better understanding of the sample's material qualities.

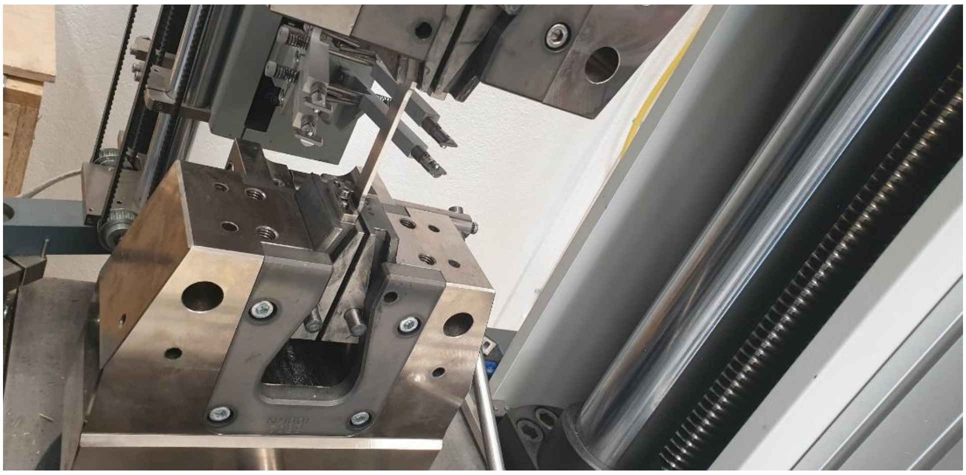

Picture 13: Securing a specimen in the tensile machine.

According to the laboratory manager, the machine was purchased by NTNU for their mechanical lab in 2010, where Zwick Roell supposedly utilized the frame of the Karl-Frank tensile machine, swapping out the mechanical components with their own (K. Kalvåg 2023, personal communication, 15 May). The machine was last inspected and calibrated by Zwick Roell in 2018.

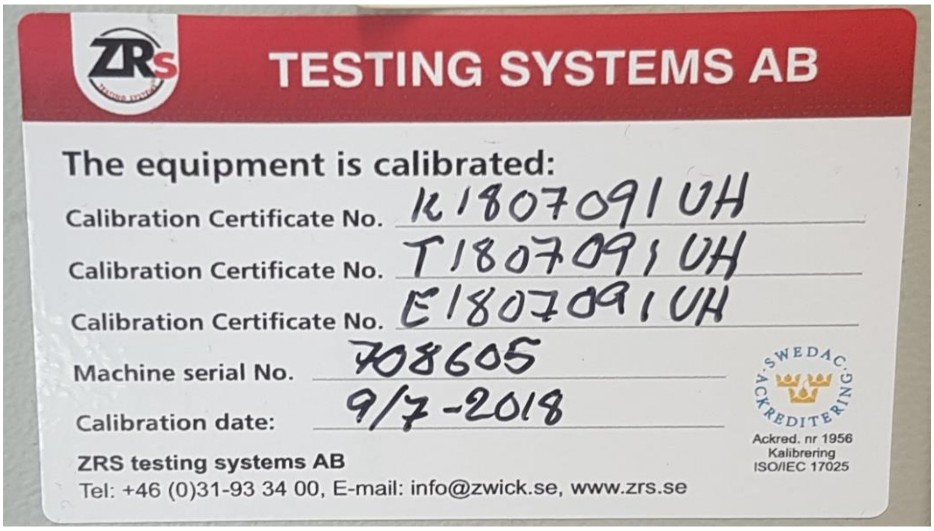

Picture 14: Certificate of calibration of Zwick 100kn machine.

4 Methodology

4.1 Specimen preparation

4.1.1 Preparation

For the tensile tests, a cylindrical block with the dimension of 110mm diameter and 72mm height was chosen. The block was machined to be flat on one side, above the required width for the grips (16mm), as can be seen in the picture below. The surface would then have been cleaned for contaminants to prepare for the LMD-printing process. Before the printing process begins, the operator goes through some preparation procedures to make sure the machine is ready. For example, the operator makes sure that the safety glass, which inserts between the laser and the printing area, is cleaned.

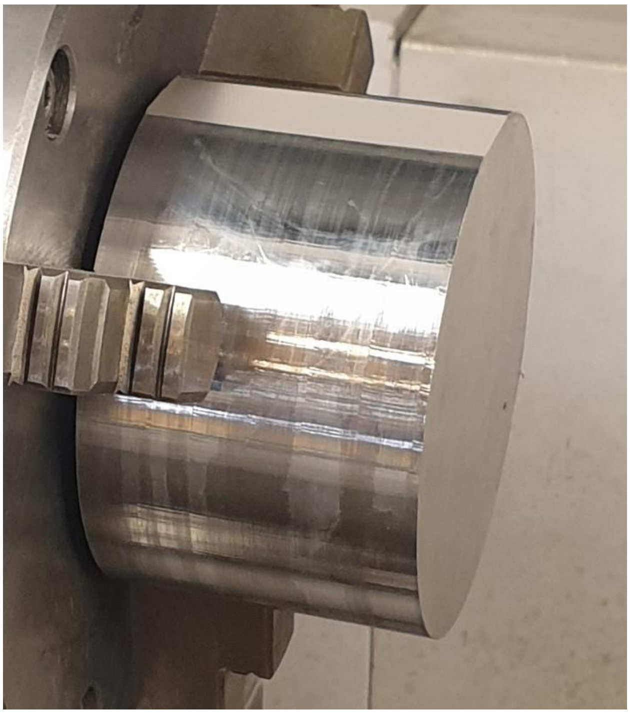

Picture 15: SDSS block ready for LMD printing. the top was machined flat.

4.1.2 Printing

The process begins with the operator inserting the steel bar in the TruLaser Cell 3000 chamber and preparing the metal powder for printing. For our printing process, the powder used is made up of very fine super duplex stainless-steel particles, which are loaded into the printer's powder delivery system (hopper). This prevents or minimizes oxidation during the printing process. Before beginning, the nozzle will stabilize itself for 20 seconds. According to the NAM technician, this is to allow the powder solution to settle prior to the print process (M. M. Vik 2023, personal communication, 3 May).

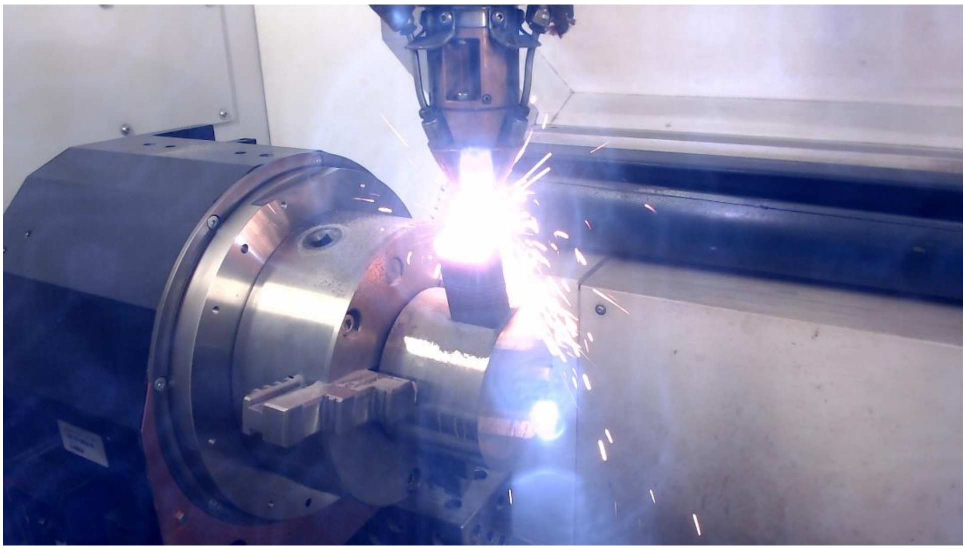

Picture 16: The specimens being printed by the TrueLaser 3000.

Next, the printer uses a precision nozzle to deposit the metal powder in thin layers onto the build platform. The nozzle is controlled by a computer program/ printer software that directs the powder deposition in a precise pattern to build our object. Once the metal powder is applied, a high-powered laser is used to melt the SDSS particles and fuse them together. The laser is guided by advanced optics and the printer's computer control, which controls its intensity and movement to ensure that the powder is melted in a precise pattern. For this particular build, the technician stated that they added a 5-second pause per layer (M. M. Vik 2023, personal communication, 3 May). This is to allow the part to cool down in-between layers because the geometry of the sample makes it difficult for the object to dissipate heat. This process repeats layer by layer until the object is complete. After the printing process is complete, the printed object may require polishing or heat treatment to improve its strength, durability, and surface finish.

4.1.3 Machining

After the printing process, the piece was delivered to a third-party company, SINTEF, which has machining capabilities for our desired dog bone specimens. The usual machining process involves cutting, machining the taper, deburring/smoothing, and measuring/verifying of the desired dimensions.

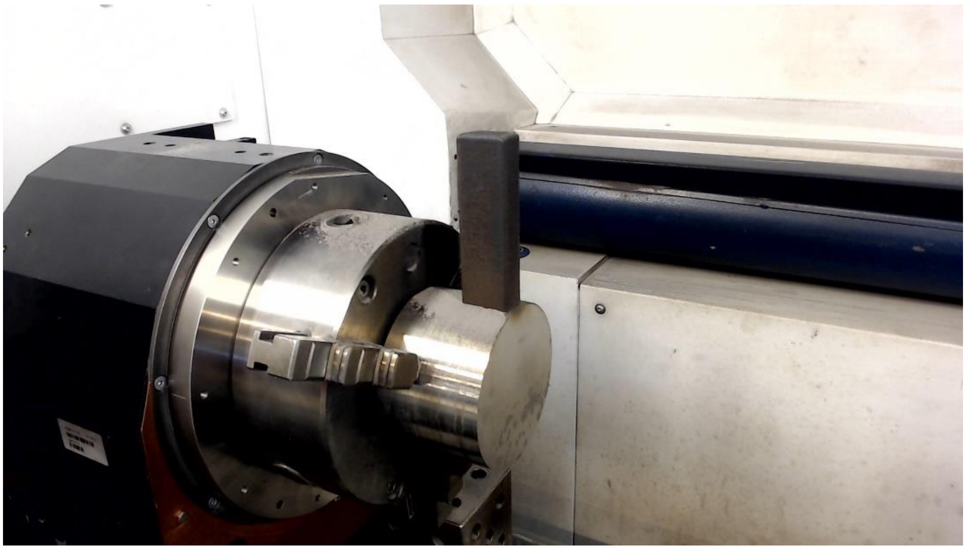

Picture 17: The final block which will be used to create tensile specimens.

A general machining process begins with cutting the piece into a rectangular shape which has a larger dimension than the final. The cutting was done by a waterjet cutter/bandsaw to achieve a clean and straight cut. After cutting, the rectangular piece was set in a milling machine to shape it to the desired dimensions. The milling machine has a library of preprogrammed tensile specimens (with different types of standards) where you can choose your sizing. Once you are done with the inputs, the machine can grind the desired dimensions. (TensileMill CNC, 2019)

The Next step is smoothing, the specimen can have some sharp edges or irregularities on its surface. By using sandpaper, it can be easily smoothened. While smoothing we should pay attention to the integrity and dimensions of the specimen. This can be checked by using calipers. After that, the specimen is ready for tensile testing.

Picture 18: The machined specimen.

4.2 Mechanical Testing

4.2.1 Set up of tensile test machine

Before we started testing, the lab technician had installed the inserts with the right size for our specimen size and set the machine to a neutral position by zeroing the load cell. Before any specimens could be inserted, they would have to be measured with an electronic caliper, and their average values calculated. Below are the measurements for the tensile specimens.

# (UNS S32750)	Thickness (mm)	Width (mm)	Cross-Sectional Area (mm^2)
1	2.96	12.54	37.12[1]
2	2.94[1]	12.56[1]	36.93[1]
3	2.94 [1]	12.54	36.87[1]

Table 1: Measurements before testing the tensile specimen, [1] numbers rounded to 2 decimals.

Then the operator inputs the dimensions of the specimen, which the machine used to calculate the output data we wanted. After the measurement, the data acquisition and recording software was activated and the material corresponding to the specimen was selected in the software. By resetting the load cell, the load frame could only be set to measure only the magnitude of the force (load) being exerted on the specimen. Grippers were adjusted to fit the size of the specimen. This was followed by attaching extensometers to the reduced area of the test specimen, at exactly 20mm around the centerline. To prevent the specimen from slipping, inserts were used to preload the machine. After the specimen was removed, the extensometers were adjusted to zero values and the test began to measure the strain on the specimen. The data was recorded by the software on the spreadsheet. By placing the sample in that tensile machine, the tensile test was performed, and the results were recorded on the computer, where they could be analyzed later.

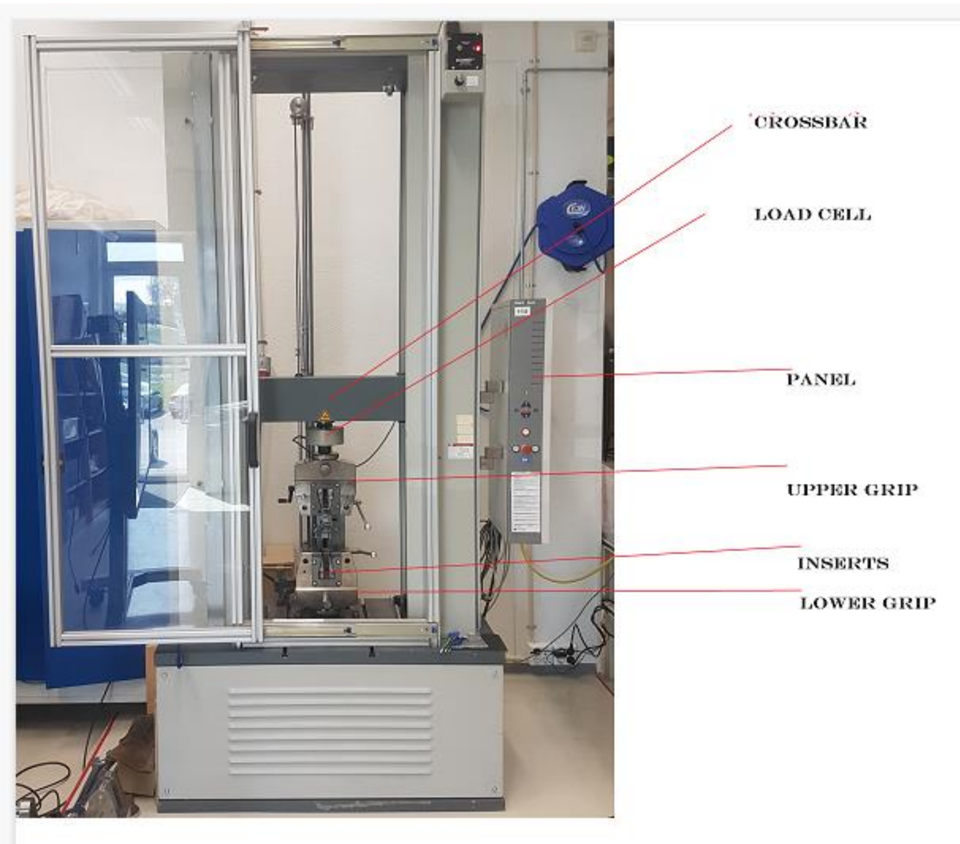

Picture 19: Components of a tensile machine.

5 Results

5.1 Missing values in the test data

When reading through the resulting data from the tests, missing values were found in specimen #2. The result from this test was missing Young’s modulus m_E, the offset yield strength $R_{p0.2}$ and the elongation A_g.

Going through the video footage of the tests, a potential point of failure was identified. During testing, the extensometer was attached to the middle to measure data at the weld point between the parent material and printed material. Usually, when the specimen is about to fail, the extensometers will detach just before. That did not happen in this test, as the extensometer failed to release from the sample, causing it to be forcefully ripped off when the specimen failed. It is not entirely clear if this is the primary cause of the data loss, or why it happened.

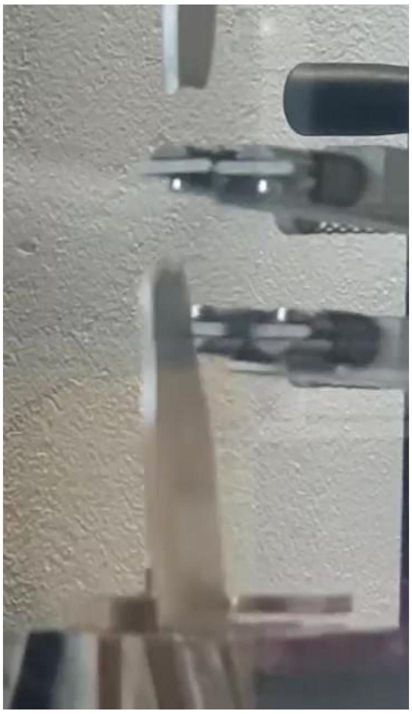

Picture 20: The extensometer attempting to hold onto a sample has already broken.

While the missing data is not critical to the analysis of these specimens, it is possible to estimate Young's modulus and the offset yield from the raw data received in the test. The elongation is not easy to estimate without proper measuring tools and is not considered critical enough for the test to be measured.

5.1.1 Calculating the missing values

In order to restore some of the results, the raw data was extracted from the Excel sheet and manual calculations were made. Manual calculations could be done for m_E and $R_{p0.2}$, whereas A_g would have to be measured, and would not be accurate enough to be useful data.

Because the values given in the Excel spreadsheet are given in direct percentages, they will first need to be converted to decimals before they can be used to calculate the values needed.

Young's Modulus

$$m_E = \frac{\sigma_2 - \sigma_1}{\varepsilon_2 - \varepsilon_2}$$

$$m_E = \frac{200.3097716 - 100.3623032}{0.00087000001 - 0.00038999999} = 208223.8838MPa$$

$$m_E = 208.2238838 \approx 208.22GPa$$

5.1.2 Graphical solution for Young's Modulus

Using the same number from the calculation as the datapoints we used in the calculations, a linear trend line was created, which has these values. This is Young's modulus, as estimated by Excel.

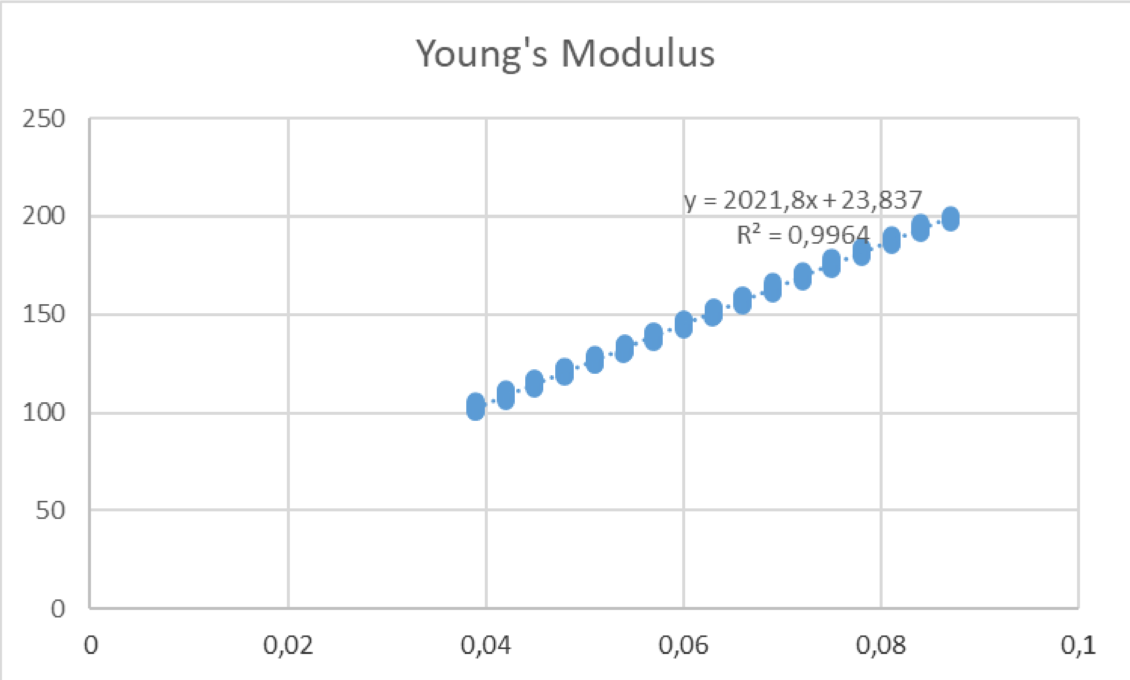

Figure 6: Graph of the linear trend line used to calculate Young's modulus of specimen #2.

Note that the units here are derived from the raw data, which measures percentages in whole numbers, not decimals. Therefore, Young's Modulus is 2021.8, or 202.18GPa. This falls much closer in line with the values of specimens #1 and #3.

5.1.3 Estimating the offset yield graphically

The 0.2% offset yield would have to be solved graphically by estimation. To find the 0.2% offset line, offset strain and offset stress was calculated from the original strain and standard force using Young's Modulus found graphically. This would create a line going parallel to the original linear portion of the stress/strain curve. To find the intersection between both graphs, a horizontal line using simple xy-coordinates was used. With this line, it is estimated that the offset yield strength lies roughly at 652MPa. This aligns somewhat with the results observed in specimens #1 and #3.

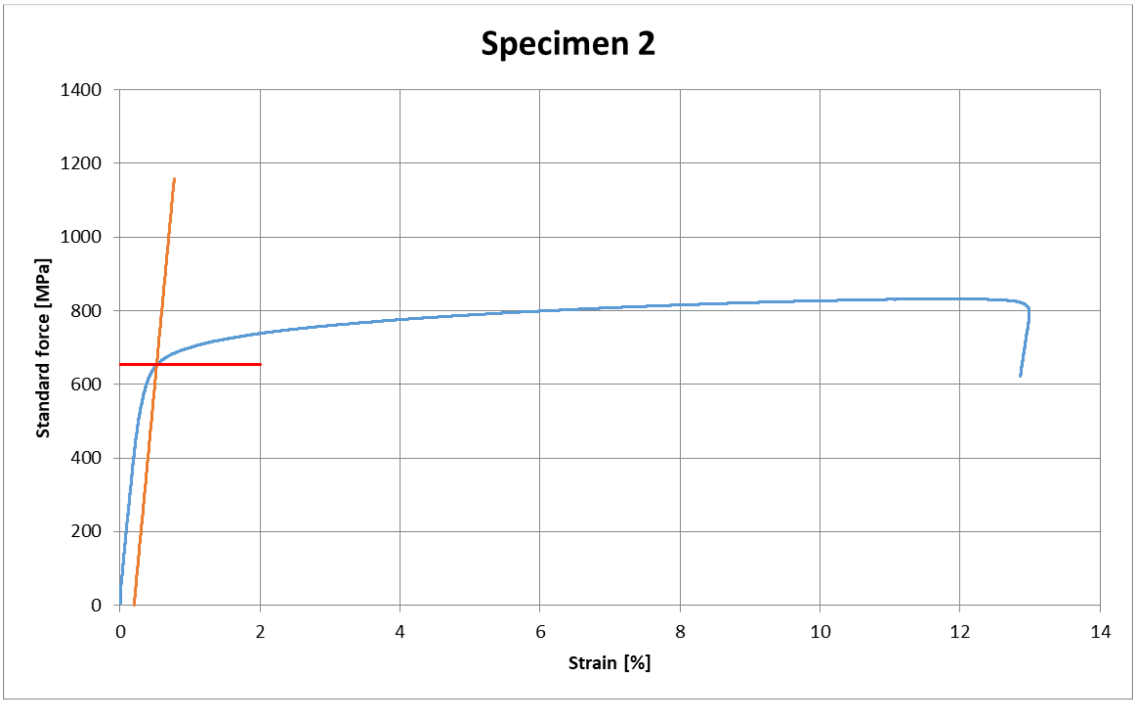

Figure 7: Graph of the intersect line used to find the offset yield.

5.2 Final results

5.2.1 Raw data & computer-generated report

All the results were compiled into a report by the testXpert program. The data recorded by the program is shown below.

Statistics:

Series n = 3	m_E GPa	$R_{p0.2}$ MPa	R_{eH} MPa	R_{eL} MPa	R_m MPa	F_m kN	A_g %	a_0 mm	b_0 mm	S_0 mm²
$\bar{x}$	199	639	-	-	827	30,59	8,68	2,947	12,55	36,97
s	1	7	-	-	4	0,17	1,91	0,01155	0,01155	0,13
ν [%]	0,41	1,03	-	-	0,48	0,54	21,97	0,39	0,09	0,35

Picture 21: Statistic table as according to the computer-generated report

Do note that the data shown above is derived directly from the software report and does not account for the missing data we recovered. The averages calculated in m_E, $R_{p0.2}$, and A_g do not correspond to all data shown but only data from specimens #1 and #3.

5.2.2 Appended report

Here is the data as recorded when the missing numbers are accounted for. The averages of x were calculated for m_E and $R_{p0.2}$, but not A_g.

Series n=3	m_E GPa	$R_{p0.2}$ MPa	R_m MPa	F_m kN	A_g %	A_0 mm	b_0 mm	S_0 mm^2
x	~200	~643	827	30.59	8.68	2.947	12.56	36.97
s	1	7	4	0.17	1.91	0.0116	0.0116	0.13
v [%]	0.41	1.03	0.48	0.54	21.97	0.39	0.09	0.35

Table 2: Appended statistics table, red marks incomplete data.

Some data is still incomplete on this table, though they are accurate enough to be kept. Below is the graph of all 3 specimens compared to each other, comparing the three.

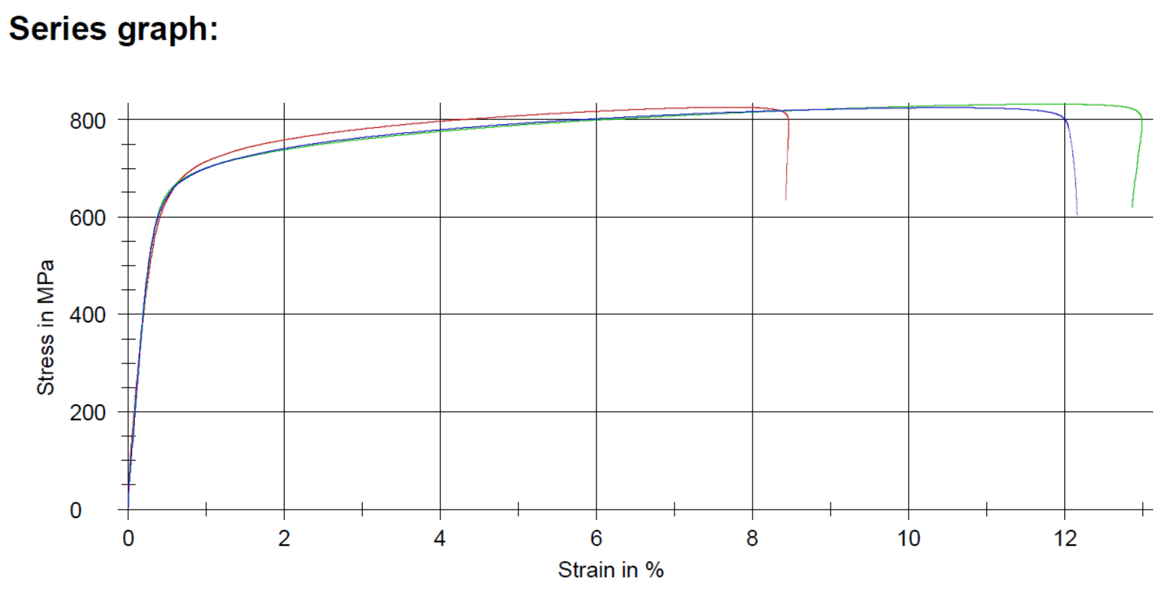

Figure 8: Graph comparing the stress/strain curve of all 3 specimen.

Specimen #1 had the lowest stress/strain curve of all the samples, with failure starting at roughly 8.5% strain, whereas specimens #2 and #3 reach a strain of 13% and 12% respectively. The stress/strain curve travels very far on the x-axis, with a waterfall at the end. This suggests that the specimens absorbed a lot of energy before eventually failing, which suggests a ductile, or semi-ductile failure.

5.2.3 Specimen #1

The computed mechanical properties of repaired specimen #1 are presented in the table below. These properties show insights into the mechanical integrity and performance of the repaired area.

m_E (GPa)	$R_{p0.2}$ (MPa)	R_m (MPa)	F_m (kN)	A_g (%)	a_0(mm)	b_0 (mm)	S_0 (mm^2)
198	634	826	30.65	7.33	2.96	12.54	37.12

Table 3: Results of specimen #1

The ultimate tensile strength of this specimen was measured at 826MPa, which is much greater than the expected minimum value of 750MPa. Similarly, the offset yield strength is much greater, exceeding the expected minimum value of 550MPa by almost a hundred MPa.

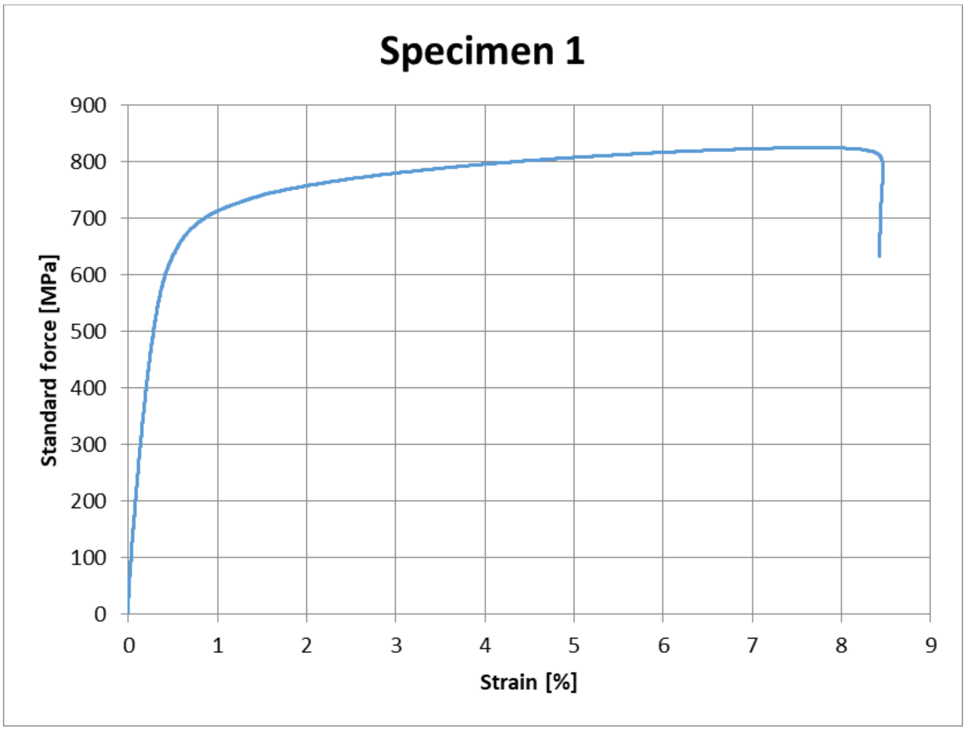

Figure 9: Stress/Strain curve graph of specimen #1.

The most noteworthy of the results is the location of the failure in the specimen. The failure was under the gauge length of the specimen, where the part is not printed. The topography of the fracture seems characteristic of a semi-ductile fracture, which is what we expected from that area of the material.

Picture 22: Fracture of specimen #1

5.2.4 Specimen #2

Shortly after the first specimen, the next was measured and inserted into the machine. The test yielded the following results.

m_{E} (GPa)	$R_{p0.2}$ (MPa)	R_{m} (MPa)	F_{m} (kN)	A_{g} (%)	a_{0}(mm)	b_{0} (mm)	S_{0} (mm^2)
~202.18	~652	832	30.72	-	2.94	12.56	36.93

Table 4: Results of specimen #2. note the missing data.

The manual calculations were inserted into the table to compensate for the missing data. Interestingly, this specimen took the longest time to break, with the test lasting for a duration of roughly three and a half minutes. This somewhat corresponds with the strain curve, which tops out at 13%, which is the highest strain of the three samples.

Figure 10: Stress/Strain curve graph of specimen #2. Note the significantly longer strain curve.

Picture 23: Fracture of specimen #2

Similar to specimen #1, this specimen also suffered a failure in the lower region of the gauge length, where the parent material is located, while the printed material remained unaffected. The topography of the fracture appears ductile or semi-ductile and has signs of necking near the failure point.

5.2.5 Specimen #3

The final specimen yielded these results.

m_E (GPa)	$R_{p0.2}$ (MPa)	R_m (MPa)	F_m (kN)	A_g (%)	a_0(mm)	b_0 (mm)	S_0 (mm^2)
199	643	825	30.40	10.03	2.94	12.54	36.87

Table 5: Results of specimen #3

This test suffered similar strain to the specimen #2, but the ultimate tensile strength lies more in line with specimen #1. The test duration was similar to the first test, with a time of roughly one and a half minutes. The elongation and offset yield strength is slightly greater than in specimen 1.

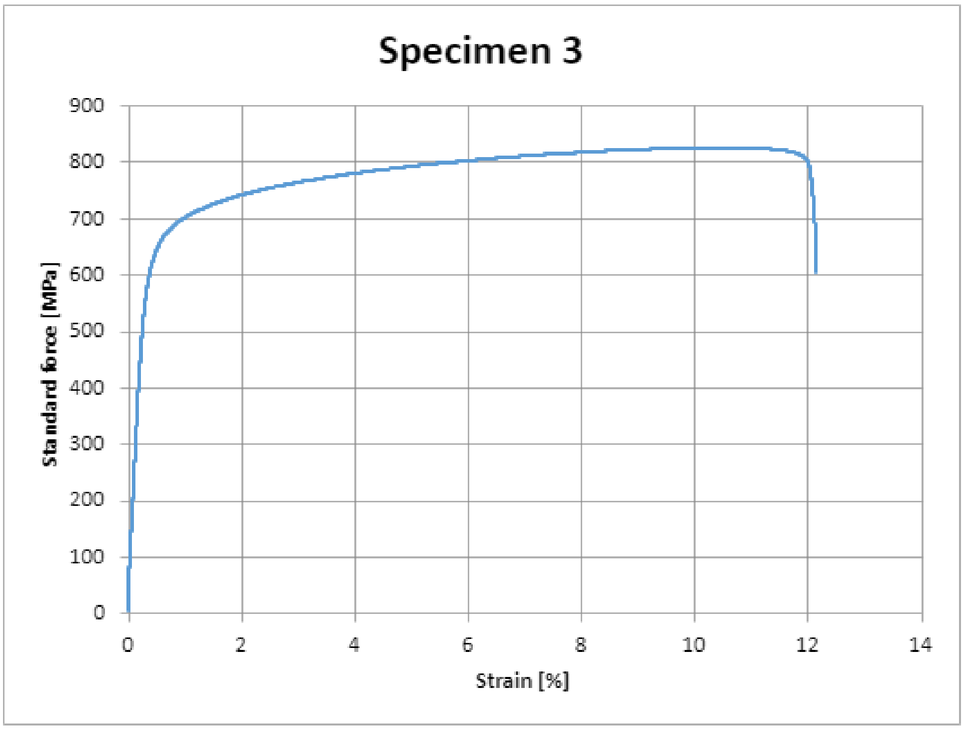

Figure 11: Stress/Strain curve graph of specimen #3

Specimen #3 suffered a failure at a similar point to the other two, lower in the sample where the round steel bar material is located, confirming that the area of failure is likely not a coincidence, but a pattern. Similar to both previous samples, the specimen experienced a semi-ductile fracture in the lower region.

Picture 24: Fracture of specimen #3

6 Discussion

6.1 Analysis

6.1.1 What the results indicate

The average tensile strength of the specimens was measured at 827MPa, which is very high compared to the value expected, at a minimum of 750MPa. However, the tensile properties of the specimen stay within a reasonable range of what is expected from hot rolled round bar steel. The offset yield strength values are also very high and show that the repaired area can withstand forces up to 639MPa without suffering plastic deformation and retains its structural integrity well beyond the minimum requirements of 550MPa.

However, going beyond the numbers, the location of the fractures on all the samples is what is most interesting. Of all three specimens tested, each and everyone had a fracture located in the lower half of the specimen, where the parent material is located. This would suggest that the printed material and the binding between the two materials are stronger than the parent material, causing the parent material to be at the point of failure.

Picture 25: All specimens after fracture. Note the necking in all samples.

The fractures in all specimens were also more ductile in nature, as shown by the graphs in 5.1, as well as the topography of the failure points on the specimens. A ductile or semi-ductile fracture is what was expected of the parent material, and also indicates that the parent material has not been embrittled by the printing process. Because there was no failure on the upper half, where the printed material is located, there is no way to say anything about the material qualities of the printed material in the sample, and therefore no conclusions that can be drawn on whether the printed material is more or less brittle than the parent material.

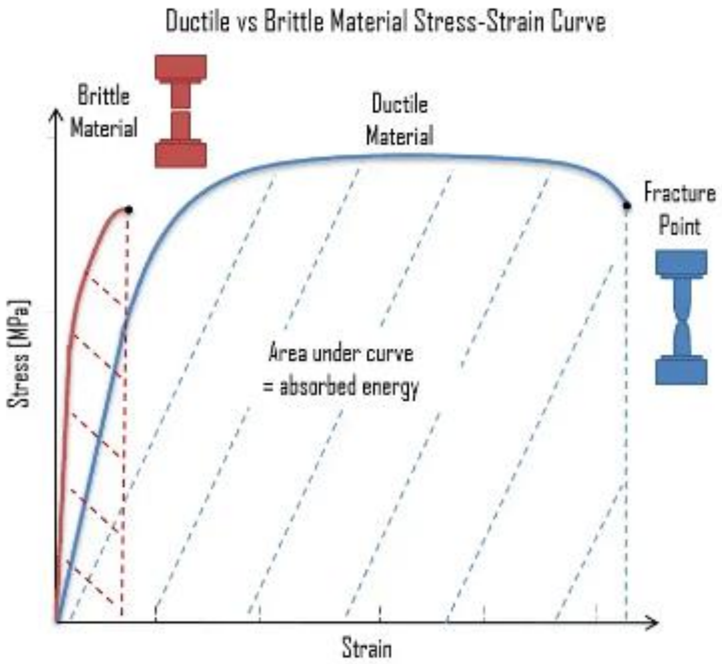

Picture 26: Ductile vs brittle material stress-strain curve (Nuclear-power.com, 2013)

Finally, there is the consideration of the values in elongation. The average elongation A_g is listed as 8.68%. This would be incredibly low for the material, and below the expected minimum of 25%. However, this number is most likely as a result of the location of the extensometers.

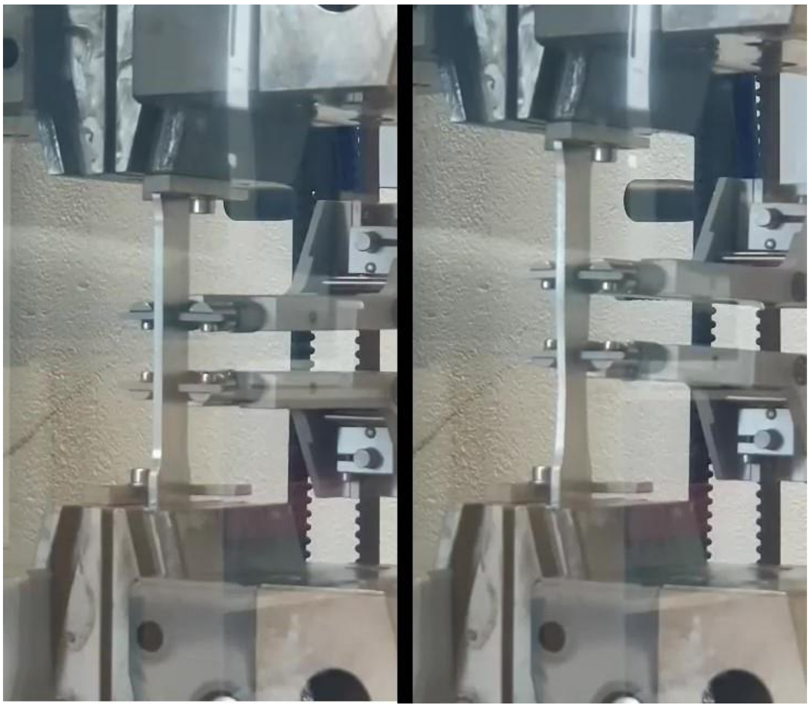

Picture 27: Elongation in sample #3 at the start and end of the experiment.

One of the bigger concerns was that the binding between the parent material and the printed material, the weld point, would be the main point of weakness. Because of this, the plan for this test was to have a more detailed picture of what happens near the weld point on the specimen. Therefore. the extensometers were situated roughly 20mm apart near the centre, which is fairly close compared to normal tensile tests. This is likely the cause of the low elongation numbers seen in the results. Because the parent material is where the majority of the elongation happens, the extensometers most likely did not pick these numbers up. Whether or not this suggests that the printed material is more brittle, or simply has a way higher tensile and yield strength compared to the parent material, is unclear.

6.1.2 More information is required.

The tensile test performed for this paper suggests that LMD-printers can create material with sufficient tensile and yield strength to hold up to regular SDSS. However, there were many other mechanical properties that could not be tested within the span of a simple bachelor thesis. Given more time and resources, it would have been ideal to test further mechanical properties, such as the ductility of LMD-printed material. It is hard to say for sure how many of the original mechanical properties are kept when utilizing additive processes.

Additionally, while the point of interest of this study was mechanical testing, it is important to acknowledge that other factors such as corrosion resistance should also be considered in practical applications. SDSS is generally used in corrosive environments and making sure that the repaired surfaces maintain their corrosion resistance is vital. Future research should look at the corrosion properties of the repaired surfaces through appropriate testing methods to provide a complete evaluation of their performance in real-world conditions. In addition, extra experiments/ tests should be considered, such as hardness measurements and the Charpy impact test, to get a more characterization of the repaired parts.

Further research is needed to optimize the AM process parameters and investigate the long-term durability of the repaired surfaces. Fine-tuning the parameters of the printing process could further enhance the quality of mechanical properties in the repaired material. Moreover, comparing the economic feasibility and scalability of using additive manufacturing for huge repair applications in the industry could provide valuable insights for its practical implementation. Further research into applying specific HM repair procedures with step-by-step processes, guidelines, and standards will improve the efficiency of hybrid methods.

6.1.3 Qualifying LMD for hybrid repair

Given the results given by previous papers on the subject matter, as well as the results of the tensile tests performed in this paper, it is not difficult to suggest that LMD-based printing as a technology is worth pursuing further. However, the question remains whether or not it is worth pursuing as a candidate for a HM method, and whether there is a possibility of qualifying the process for repairing SDSS.

Given the limited number of tests conducted in this paper, it is difficult to say with absolute certainty that all the material qualities of SDSS are kept when performing LMD-printing. However, the results gathered from the tensile tests have shown that the method has a lot of promise. There is a strong possibility that the method can be qualified in the very near future.

In terms of cost, considering the potential reduction in time and cost of repair if a HM repair process were to be implemented, qualifying LMD-printing for hybrid repair processes will likely be very lucrative in the long term, and is therefore most likely worthwhile pursuing further.

7 Conclusion

In this study, the viability of repairing SDSS with additive methods was investigated. The investigation involved creating potential repair procedure methods to be used in repairing defects on the SDSS. Various factors such as precision, deformation, clearance, surface preparation, and finish, were considered in the selection process of both methods and considerations for the repair procedure.

For repairing, two defect repair solutions were proposed, the fill method and the negative method. These proposed solutions were discussed with the technicians operating the LMD printer at NAM, who verified the possibility of their implementation into practical use. By further evaluating the practicality of implementing these methods, these methods can simplify the repair process of SDSS parts. Further development of the method could result in the creation of a standard that can be used to define the repair process step-by-step.

A series of three tensile tests were performed to evaluate some of the material qualities of a repaired piece and determine the effectiveness of the LMD-printing as a viable AM tool for a hybrid repair process. The results demonstrated that the repaired specimens exhibited greater tensile and yield strength than the minimum requirements of the parent material while being able to retain its binding. These findings suggest LMD-printing is capable of creating SDSS (UNS S32750) with similar mechanical properties to its cast & wrought counterparts.

In the end, hybrid manufacturing can be a promising technology for repairing SDSS components with exceptional precision. But additional research, testing, and assessment will be necessary to further validate the idea of using HM and determine its suitability for the specific manufacturing and repairing process.

Literature list

- American Cladding. (2022). What's the Difference Between Laser Metal Deposition and 3D Printing? [online] Available at: https://americancladding.com/whats-the-difference-between-laser-metal-deposition-and-3d-printing/ [Accessed 3 May 2023].

- Aref Yadollahi, Nima Shamsaei, Thompson, S.M. and Seely, D. (2015). Effects of process time interval and heat treatment on the mechanical and microstructural properties of direct laser deposited 316L stainless steel. [online] 644, pp.171–183. doi. Available at: https://doi.org/10.1016/j.msea.2015.07.056. [Accessed 01 May 2023]

- Dassault Systèmes. (2022). user. [online] Available at: https://www.3ds.com/make/solutions/blog/additive-vs-subtractive-manufacturing [Accessed 04 May 2023].

- DNV. (2023). *DNV-ST-B203 Additive manufacturing of metallic parts - DNV.* Available at: https://www.dnv.com/oilgas/download/dnv-st-b203-additive-manufacturing-of-metallic-parts.html [Accessed 19 May 2023].

- Ferreira, E., Dal, M., Colin, C., Marion, G., Gorny, C., Courapied, D., Guy, J. and Peyre, P. (2020). Experimental and Numerical Analysis of Gas/Powder Flow for Different LMD Nozzles. [online] 10(5), pp.667–667. doi. Available at: https://doi.org/10.3390/met10050667. [Accessed 21.0.5.2023]

- Gruber, H., Henriksson, M., Eduard Hryha and Nyborg, L. (2019). Effect of Powder Recycling in Electron Beam Melting on the Surface Chemistry of Alloy 718 Powder. [online] 50(9), pp.4410–4422. doi. Available at: https://doi.org/10.1007/s11661-019-05333-7. [Accessed 21.05.2023]

- Hall, M. (2015). Agile. [online] Agile. Available at: https://agilescientific.com/blog/2015/2/9/what-is-anisotropy [Accessed 14 May 2023].

- Hubs. (2023). What is metal 3D printing and how does it work? | Hubs. [online] Available at: https://www.hubs.com/knowledge-base/introduction-metal-3d-printing/ [Accessed 3 May 2023].

- Industrial Metallurgists. (2016). Residual Stress - Industrial Metallurgists. [online] Available at: https://www.imetllc.com/residual-stress/ [Accessed 07 May 2023].

- NIST. (2022). Additive Manufacturing/3D Printing | NIST. [online] Available at: https://www.nist.gov/mep/additive-manufacturing3d-printing [Accessed 01 May 2023].

- Noyan, I.C. and Cohen, J.B. (2013). Residual Stress. SpringerLink. [online] doi. Available at: https://doi.org/10.1007-978-1-4613-9570-6 [Accessed 19 May 2023]

- Nuclear-power.com. (2013). Available at: https://www.nuclear-power.com/nuclear-engineering/materials-science/material-properties/ductility/ [Accessed 21 May 2023].

- ResearchGate. (2018). Figure 1. Schematic diagram of the selective laser melting (SLM) process. [online] Available at: https://www.researchgate.net/figure/Schematic-diagram-of-the-selective-laser-melting-SLM-process_fig1_326891428 [Accessed 11 May 2023].

- Smithmetal.com. (2020). UNS S32750. [online] Available at: https://www.smithmetal.com/uns-s32750.htm [Accessed 01 May 2023].

- Standard.no. (2019). *NS-EN ISO 6892-1:2019. Metalliske materialer Strekkprøving, Del 1: Metode for prøving* Available at: https://www.standard.no/no/Nettbutikk/produktkatalogen/Produktpresentasjon/?ProductID=1122592 [Accessed 19 May 2023].

- Standard.no. (2016). *ISO 148-1:2016 Metalliske materialer Charpy-skårslagprøving, Del 1: Prøvingsmetode.* Available at: https://www.standard.no/no/Nettbutikk/produktkatalogen/Produktpresentasjon/?ProductID=853814 [Accessed 19 May 2023].

- Team Xometry (2022). All About Electron Beam Melting (EBM) 3D Printing. [online] Xometry.com. Available at: https://www.xometry.com/resources/3d-printing/electron-beam-melting/#:~:text=EBM%20printing%20is%20generally%20less,result%20in%20rougher%20surface%20finishes. [Accessed 4 May 2023].

- TensileMill CNC (2019). TensileMill CNC Classic - Preparing Flat Tensile Specimens. YouTube. Available at: https://www.youtube.com/watch?v=jC4oU242SMI [Accessed 20 May 2023].

- Trumpf.com. (2020). TruLaser Cell 3000 | TRUMPF. [online] Available at: https://www.trumpf.com/en_INT/products/machines-systems/laser-welding-systems-and-the-arc-welding-cell/trulaser-cell-3000/ [Accessed 19 May 2023]

- Voxeljet. (2022). Selective Laser Melting & Metal 3D Printing | voxeljet. [online] Available at: https://www.voxeljet.com/additive-manufacturing/3d-printing-processes/selective-laser-melting/#:~:text=In%20the%20SLM%203D%20printing,support%20structures%20in%20most%20cases. [Accessed 8 May 2023].

- Washington.edu. (2017). Troubleshooting and Calibration - UW Maker - UW-IT Wiki. [online] Available at: https://wiki.cac.washington.edu/display/Maker/Troubleshooting+and+Calibration [Accessed 21 May 2023].

Appendices

A. Pre-project for bachelor thesis, in Norwegian
   [forprosjekt.pdf]

B. Computer generated report for tensile test series, made by testXpert
   [3Dprinted_dogbone_6892_RomTemp - 2023-05-15_50mm test lenge.pdf]

C. Raw data from tensile tests, made by testXpert
   [3Dprinted_dogbone_6892_RomTemp - 2023-05-15_50mm test lenge.xls]

D. Repaired raw data for Specimen #2
   [Raw Data 50mm Specimen 2 Repaired.xls]

E. Video recording of tensile test: specimen #1
   [Tensile test Specimen 1.mp4]

F. Video recording of tensile test: specimen #2
   [Tensile test Specimen 2.mp4]

G. Video recording of tensile test: specimen #3
   [Tensile test Specimen 3.mp4]

H. Video footage of NAM printer at work
   [NAM Printer Video Footage (Warning - Loud).mp4]

Attachments

NAM VISIT

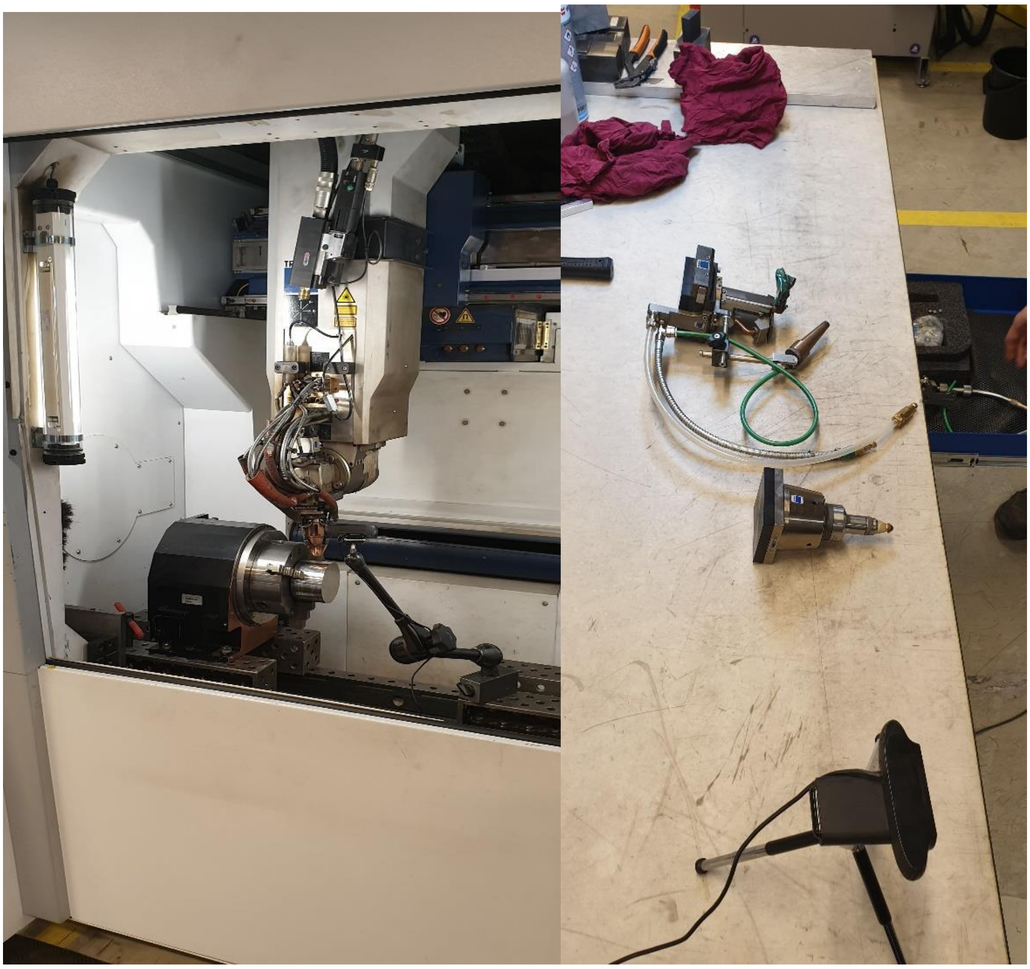

1. Different types of nozzles

2. A 3D printed rectangular block with a mixture of three types of metals

3. The plastic container which the powder of SDSS was stored in.

LAB-EXERCISE

1. Stamp of a manufacturing company for tensile test

2. The thickness of a specimen before tensile test

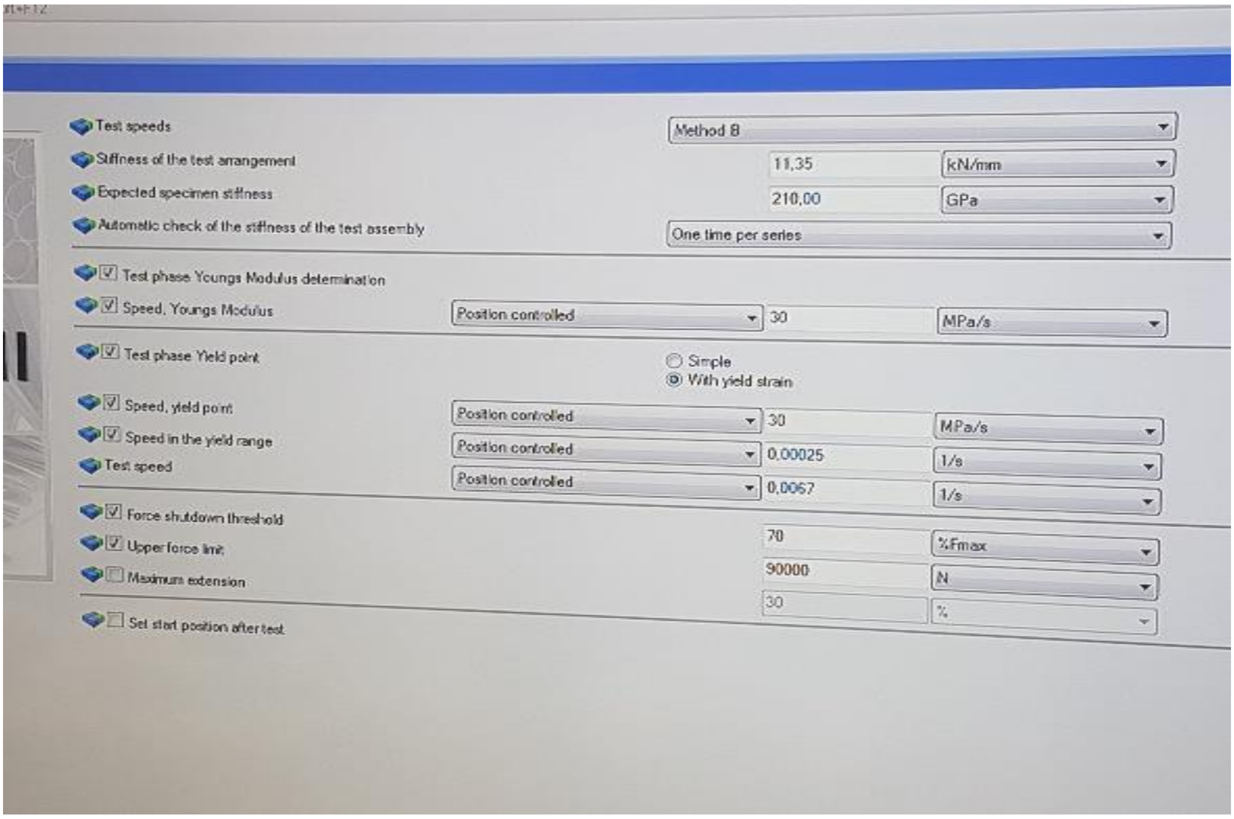

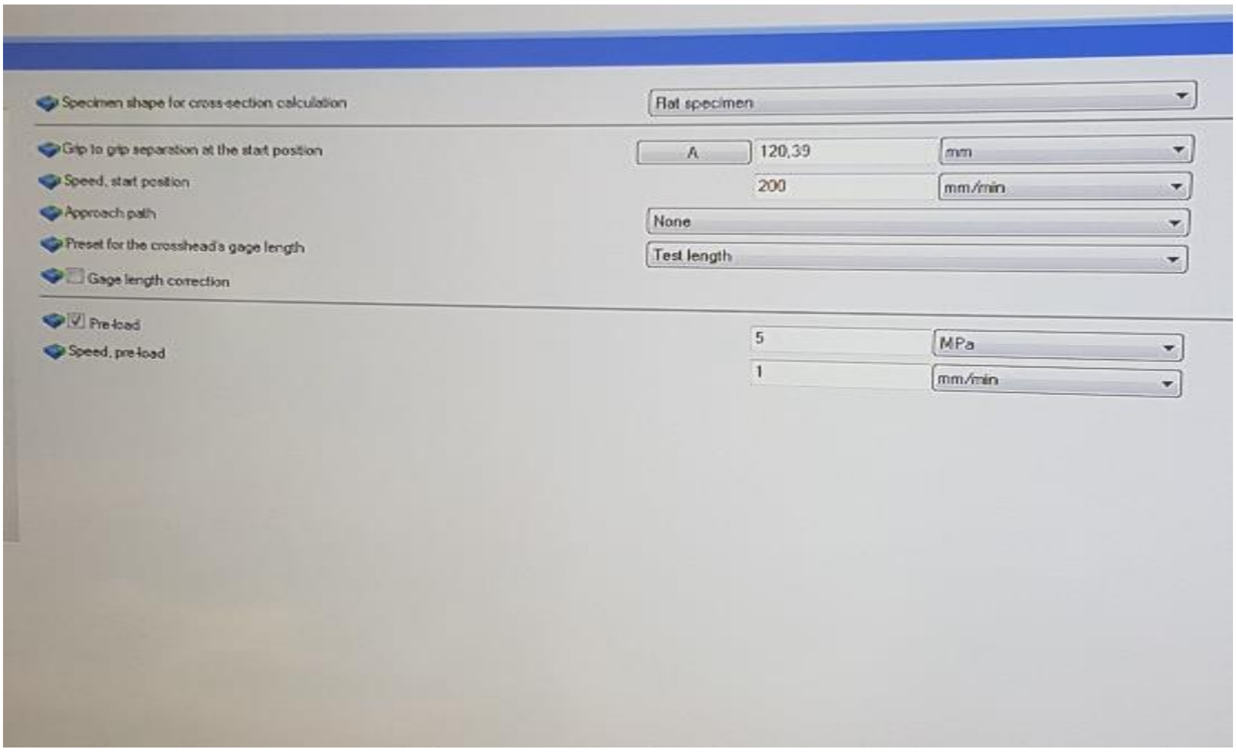

3. Different values that has been used in the tensile machine